View metadata, citation and similar papers at core.ac.uk

brought to you by CORE

provided by UNT Digital Library

SANDIA REPORT
SAND2004-0912
Unlimited Release
Printed April 2004

Experimental Investigation of Burnup Credit for Safe Transport, Storage, and Disposal of Spent Nuclear Fuel

Final Report

Nuclear Energy Research Initiative Project 99-0200

Gary A. Harms, Paul H. Helmick, John T. Ford, Sharon A. Walker, Donald T. Berry, and Paul S. Pickard

Prepared by
Sandia National Laboratories
Albuquerque, New Mexico 87185 and Livermore, California 94550

Sandia is a multiprogram laboratory operated by Sandia Corporation, a Lockheed Martin Company, for the United States Department of Energy under Contract DE-AC04-94AL85000.

Approved for public release; distribution is unlimited.

Issued by Sandia National Laboratories, operated for the United States Department of Energy by Sandia Corporation.

NOTICE: This report was prepared as an account of work sponsored by an agency of the United States Government. Neither the United States Government nor any agency thereof, nor any of their employees, nor any of their contractors, subcontractors, or their employees, makes any warranty, express or implied, or assumes any legal liability or responsibility for the accuracy, completeness, or usefulness of any information, apparatus, product, or process disclosed, or represents that its use would not infringe privately owned rights. Reference herein to any specific commercial product, process, or service by trade name, trademark, manufacturer, or otherwise, does not necessarily constitute or imply its endorsement, recommendation, or favoring by the United States Government, any agency thereof, or any of their contractors or subcontractors. The views and opinions expressed herein do not necessarily state or reflect those of the United States Government, any agency thereof, or any of their contractors.

Printed in the United States of America. This report has been reproduced directly from the best available copy.

Available to DOE and DOE contractors from
Office of Scientific and Technical Information
P.O. Box 62
Oak Ridge, TN 37831
Telephone: (865)576-8401
Facsimile: (865)576-5728
E-Mail: reports@adonis.osti.gov
Online ordering: http://www.doe.gov/bridge

Prices available from (615) 576-8401, FTS 626-8401

Available to the public from
U.S. Department of Commerce
National Technical Information Service
5285 Port Royal Rd
Springfield, VA 22161

Telephone: (800)553-6847
Facsimile: (703)605-6900
E-Mail: orders@ntis.fedworld.gov
Online order: http://www.ntis.gov/help/ordermethods.asp?loc=7-4-0#online

SAND2004-0912
Unlimited Release
Printed March 2004

Experimental Investigation of Burnup Credit for Safe Transport, Storage, and Disposal of Spent Nuclear Fuel

Final Report

Nuclear Energy Research Initiative Project 99-0200

Gary A. Harms and Paul H. Helmick
Applied Nuclear Technologies
John T. Ford
Nuclear Reactor Facilities
Sharon A. Walker
Facility Engineering and Support
Donald T. Berry
Hot Cells and Gamma Facilities
Paul S. Pickard
Advanced Nuclear Concepts

Sandia National Laboratories
P. O. Box 5800
Albuquerque, NM 87185

Abstract

This report describes criticality benchmark experiments containing rhodium that were conducted as part of a Department of Energy Nuclear Energy Research Initiative project. Rhodium is an important fission product absorber. A capability to perform critical experiments with low-enriched uranium fuel was established as part of the project. Ten critical experiments, some containing rhodium and others without, were conducted. The experiments were performed in such a way that the effects of the rhodium could be accurately isolated. The use of the experimental results to test neutronics codes is demonstrated by example for two Monte Carlo codes. These comparisons indicate that the codes predict the behavior of the rhodium in the critical systems within the experimental uncertainties. The results from this project, coupled with the results of follow-on experiments that investigate other fission products, can be used to quantify and reduce the conservatism of spent nuclear fuel safety analyses while still providing the necessary level of safety.

Acknowledgements

The work described in this report was funded as Nuclear Energy Research Initiative project 99-0200 under IWO M9SF99-0200.

It takes a village, and not a small one, to raise a reactor. The work reported here would not have been possible without the efforts of a large number of individuals in different roles. The lead roles on the project team were taken by Gary Harms, Sharon Walker, Paul Helmick, John Ford, and Don Berry. The team included Matt Burger, Sid Domingues, Jim Fisk, Francisco Gonzalez, Jim Andazola, Gerald Naranjo, Mike Torneby, Jim Duncan, Dee Brock, Sylvia Gomez, Kevin Cooley, David Samuel, Kevin McBride, Tom Vanderbeek, Bill Peters, Dave Mills, Rob Naegeli, Joe Padilla, Tony Zamora, Rick Anderson, Manny Trujillo, Warren Strong, Laura Latoma, Fernando Dominguez, Dave Vehar, Tracy Dunham, and Freddie Davis. The management team included Paul Pickard, Jeff Philbin, Jim Bryson, Ted Schmidt, Jack Loye, Ron Simonton, and Ken Reil. Philip Cooper and Edward Parma, Jr. provided thoughtful comments on the manuscript. Emily Fuller gave patient assistance in the formatting and release of this document. Madeline Feltus of DOE NE-20 was instrumental in getting the special fuel elements built.

Table of Contents

List of Figures

List of Tables

1. Executive Summary

1.1. Research Objectives

The Nuclear Energy Research Initiative funded a critical experiment focused on burnup credit issues at Sandia National Laboratories as project 99-0200. This is the final report of that project. The project has two products: a critical experiment capability was established at Sandia that is now available to perform critical experiments with low-enriched fuel and benchmark criticality measurements were made that can be used to test the methods and data employed in the criticality safety analyses of shipping, storage, and disposal of spent nuclear fuel.

Burnup credit is the process of accounting for the decrease in the reactivity of nuclear fuel produced by the changes in the fuel actinide concentrations and the buildup of fission product absorbers caused by the burning of the fuel. To apply burnup credit safely, the methods used in its application must be validated: the fuel isotopic composition in the burned state must be accurately predicted, and the neutron multiplication of spent fuel configurations must be accurately predicted. This project addresses the second part of the validation issue.

A critical assembly with low-enriched UO_2 fuel representative of light water reactors was built at Sandia. The assembly concept is shown in Figure 1-1. The figure shows a cut-away view of the assembly core and shows conceptually how experiment materials are inserted into the assembly. It also includes a photograph of one of the critical configurations of the assembly.

The assembly consists of a water-moderated array of driver fuel elements surrounding a smaller number of experiment fuel elements. Test materials can be inserted between the fuel pellets in the experiment elements to allow accurate measurements of the reactivity worth of important fission products. The assembly also includes three fuel-followed control/safety elements and a fueled source element.

The benchmark data from the project are the measured critical array sizes for configurations with and without an experiment material. The critical configurations can be analyzed with criticality safety analysis codes. The difference between the calculated result and the measured result gives the bias in the code and the nuclear data. Critical experiments can be performed in the unperturbed assembly and with a test material, a fission product simulant, present in the assembly. The data from the unperturbed assembly can be used to "zero out" analysis biases due to all other sources than from the experiment material. This allows not only integral tests of the codes but also tests of the nuclear data for a specific material.

1.2. Project Synopsis

Five broad tasks were outlined in the project proposal:

- Task 1 – Obtain the necessary National Environmental Policy Act (NEPA) approvals.
- Task 2 – Prepare safety basis documentation for the experiment and obtain approvals.
- Task 3 – Design and procure the experiment hardware.

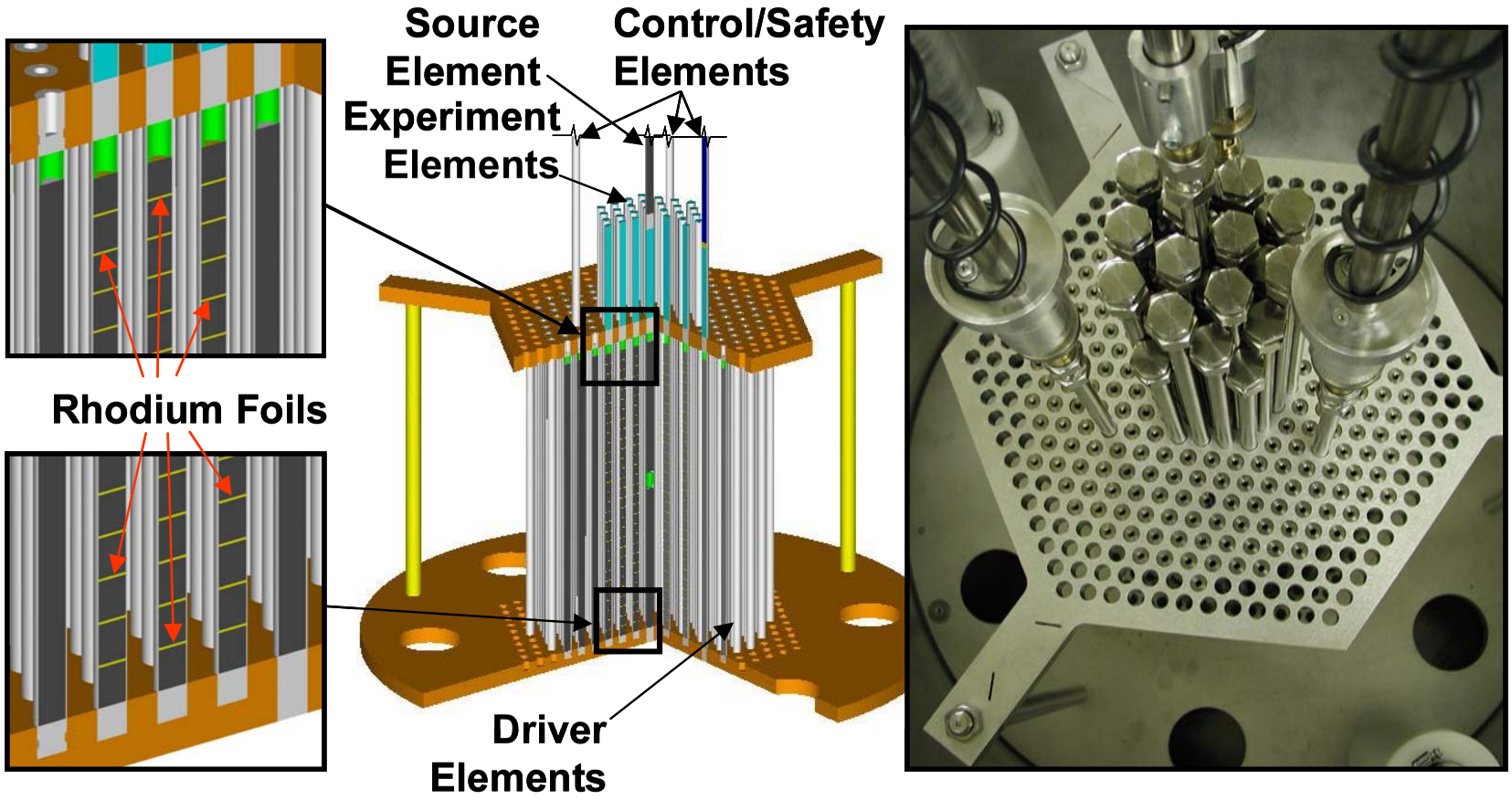

Figure 1-1. Cutaway view of the critical assembly showing the method for including experiment materials. The photographic inset shows the critical configuration of one of the experiments.

- Task 4 – Perform the benchmark experiments.
- Task 5 – Decommission and decontaminate the experiment.

The NEPA approvals for the experiment were obtained in the first year of the project. Sandia filed an Environmental Checklist/Action Description Memorandum with the Department of Energy requesting that the experiment be categorically excluded from further NEPA documentation. The exclusion was granted.

The critical experiments were performed in the reactor room of the Sandia Pulsed Reactor Facility (SPRF) in Sandia's Technical Area V. Early in the project, the determination was made that an addendum to the SPRF Safety Analysis Report (SAR) would be required to establish the safety basis for the critical experiments. The SAR addendum was completed and Technical Safety Requirements (TSR) for the operation of the critical assemblies were written. Both documents were submitted to the Sandia Internal Review and Appraisal System (SIRAS) for safety review. The SIRAS review was completed in April, 2001. The SAR addendum and the TSR were then submitted for DOE approval. The DOE approval of the SAR addendum and the TSR was received in December, 2001. A three-part readiness assessment was then initiated. The readiness assessment culminated in a review of the facility and the experiment by a DOE team in late February, 2002. Issues identified in the DOE readiness assessment team were resolved and approval to operate the critical assembly was obtained.

The design of the critical assembly hardware was completed and procurement of the non-fuel hardware was initiated in the second year of the project. The assembly hardware was received and assembled. Two grid plate sets were obtained, each with different fuel element spacing, to give different neutron spectra in the assembly. The critical assembly was controlled with the instrumentation and control system from an earlier critical experiment that was modified for this project. The driver fuel elements, which were fabricated in 1996 as part of another critical experiment, were transferred from Los Alamos National Laboratory to Sandia. The experiment fuel elements, the control/safety elements and the source elements utilize the same uranium dioxide fuel stock as used in the driver fuel fabrication. These fuel elements utilize cladding assemblies fabricated by a commercial nuclear fuel vendor and loaded with fuel pellets at Sandia.

The critical experiments performed as part of this project were designed to investigate the reactivity effect of rhodium, one of the fission products most important to burnup credit, on the assembly. Circular rhodium foils with the same diameter as the fuel pellets were obtained in three thicknesses. The foils were placed between the fuel pellets in the experiment fuel elements. First, the critical array size with only driver fuel was determined. Then the 36 fuel elements surrounding the central source element were removed and replaced with experiment fuel elements that had been "poisoned" with rhodium and the critical array size measured. Experiments with three different foil thicknesses gave data for different levels of self-shielding in the foils.

All ten of the critical experiments planned as part of the project were performed. Five experiments were conducted with each of the two grid plates: one with driver fuel only; one with experiment elements containing no poison foils; and one with each of the three sets of experiment elements loaded with rhodium foils. During each of the experiments, the critical

assembly was loaded in a sequence of steps starting with a low multiplication configuration and proceeding to progressively higher multiplication. Each step provided an updated estimate (by extrapolation) of the number of rods required to reach a critical configuration.

1.3. Results

The critical array size was measured for the ten critical experiments. The peak multiplication of the experiments ranged from 685 to 2381. All of the actual critical array sizes included a fractional fuel element estimated by extrapolation of the measured multiplication data. Knowing the critical array size and the incremental worth of the fuel elements, the eigenvalues for integral arrays was determined. The experimental uncertainty in the eigenvalues was 0.15% for the experiments performed at 2.0 cm pitch and 0.08% at 2.8 cm pitch when comparing these experiments with unrelated experiments (e.g. critical experiments not performed as part of this project). When making comparisons between the experiments in this set at a given pitch, the experimental uncertainties are reduced to 0.030% at 2.0 cm pitch and 0.040% at 2.8 cm pitch.

The results of the experiments were compared with the results from two different Monte Carlo codes widely used for criticality safety analyses. The biases between the calculations and the experiments were consistent with the biases for the same codes for other critical experiments containing low-enriched UO_2 fuel.

The real value of these experiments is in the data they provide to test the accuracy of the treatment of rhodium by the codes. Two critical configurations without rhodium were included in the experiment set for each fuel element pitch. These configurations were included to "zero out" most of the bias between calculations and experiments so the effect of the rhodium could be isolated. The reactivity worth of the rhodium in the experiments ranged from 0.97% to 3.51%. Both codes reproduced these reactivity worths within the smaller experimental uncertainties for correlated experiments.

1.4. Future Potential

In addition to producing benchmark critical measurements and data on rhodium in critical systems, this project leaves intact a capability to perform low-enriched critical experiments at Sandia. A large fraction of the project resources were expended establishing this capability. Subsequent critical experiments can use the capability with a much reduced up-front cost. There are a number of ways that this capability can be exploited. In fact, another NERI project using this capability, *Reactor Physics and Criticality Benchmark Evaluations for Advanced Nuclear Fuel* (01-124) was in progress when this report was written. Other possible uses of the critical experiment capability could be:

1. Measure the behavior of other fission products on a critical system. Such follow-on experiments could be used to provide the justification for the inclusion of fission products in the criticality analysis of spent fuel shipping, storage, and disposal configurations.
2. Measure static reactor physics parameters of critical systems with higher (e.g. >5%) enrichment such as are being done in NERI project 01-124. Such experiments could include measurements of fission density profiles, soluble poison reactivity worths, burnable poison rod reactivity worth, and others.

3. Examine the static reactivity behavior of new burnable poison types or configurations.
4. Perform critical experiments with variable enrichments to simulate the graded enrichments in BWR cores.
5. Examine cores with axially graded enrichment and possibly graded fission product content to simulate the end effects in spent nuclear fuel.
6. Perform critical experiments with Generation IV fuels and with transmutation fuels.
7. Examine the reactor physics behavior of transmutation targets.

These are examples of experiments that could be performed with the critical experiment capability established as part of this project. Many other studies are possible.

2. Introduction

The US Department of Energy Nuclear Energy Research Initiative (NERI) funded a critical experiment at Sandia National Laboratories focused on burnup credit issues. The Burnup Credit Critical Experiment (BUCCX) was used to evaluate reactivity effects of fission-product species in support of activities to establish burnup credit in handling, storage, and transport of spent nuclear reactor fuel. As fuel is burned in a nuclear reactor, its ability to sustain a fission chain reaction decreases due to the "burnup" process where the fissionable species are depleted and fission-products, some of which are strong neutron absorbers, build up. Burnup credit is the process of accounting for this decrease in the reactivity of spent nuclear fuel in criticality safety analyses. Such a credit, in allowing more fuel to be shipped in a given cask or container, can have large economic benefit by reducing both the number of casks and number of shipments required to handle a given inventory of spent reactor fuel.

To apply burnup credit safely, the methods used in its application must be validated: the fuel isotopic composition in the burned state must be accurately predicted, and the neutron multiplication of spent fuel configurations must be accurately predicted. The BUCCX addresses the second part of the validation issue. While the number of critical experiments that include the actinides important to burnup credit is significant, the database of experiments with critical systems that include single fission products is sparse. The BUCCX helps fill this gap. A critical assembly fueled by low-enriched UO_2 was built. Fission product materials were inserted into the assembly to determine the effect of the materials on array size at delayed critical. These measurements have extended the database that can be used to validate burnup credit analyses.

The BUCCX benefited from facilities and earlier work on critical experiments at Sandia. The control system and a significant amount of the assembly hardware was acquired for the Space Nuclear Thermal Propulsion Critical Experiment (CX) (SNL 1989). The CX was designed to simulate a nuclear thermal propulsion reactor and addressed design margins, controllability and accident scenarios of this type of reactor. The safety basis analysis and the assembly fuel were from the Spent Fuel Safety Experiment (Harms 1995), a critical experiment to measure the effect of spent fuel on a critical system. The BUCCX was operated in the SPRF.

The BUCCX was a fuel-replacement experiment. The critical loading of an assembly of "fresh" fuel (e.g. fuel containing only unirradiated UO_2) in a given configuration was measured. A fission product material, rhodium, was then be inserted into the assembly and the critical loading measured again. The benchmark data obtained from the experiment is the difference between the critical fuel loading with unmodified fuel and the loading with the addition of the fission product. Approximately 350 unirradiated driver fuel rods were available for the experiment. Similar in design and composition to those of a nuclear power reactor, they consisted of low-enriched uranium-dioxide pellets in Zircaloy cladding tubes that can be configured to represent the physical characteristics of such reactors.

The assembly was designed to accommodate the distribution of benign chemical simulants for specific fission-product nuclides in the assembly. The fission product simulants can be included interstitially between fuel elements or inside special assembly fuel elements designed for the purpose. Assemblies loaded with fission product simulants can be used to

study burnup effects without having to deal with the radiological complications of actual spent nuclear fuel and its associated very-high-radioactivity environment. The BUCCX design allows for a wide variety of fission-product simulants and their distributions to be studied while remaining comfortably within the safety analysis limits defined in an addendum to the SPRF Safety Analysis Report (SNL 2002a).

The assembly was designed so that the experiments were as clean as possible. The materials that have significant impact on the reactivity of the assembly were limited to materials that are present in spent nuclear fuel. The fuel is 4.31% enriched UO_2 in zircaloy cladding moderated by water and supported by aluminum grid plates. The UO_2 was used in the Critical Mass Laboratory at the Pacific Northwest National Laboratory in several experiments (for example, LEU-COMP-THERM-002) documented in the International Handbook of Criticality Safety Benchmark Experiments (NEA 2002). Small amounts of other materials, such as aluminum and polyethylene, are included in the assembly and have a small reactivity impact on the assembly.

3. Background

3.1. Project Goal

As nuclear fuel is burned, the composition of the fuel changes due to the depletion of the actinide species and the buildup of fission products. The reactivity of the fuel decreases as fissile materials are burned and fission product poisons are accumulated. Taking account of this reactivity decrease (burnup credit) allows spent nuclear fuel to be safely packed in more dense arrays in transportation, storage, and disposal configurations than would be possible if the composition changes were ignored. Allowing such burnup credit will result in significant cost savings in the handling of spent nuclear fuel while maintaining the required level of safety.

A key issue related to acceptance of spent fuel burnup credit is the verification of the impact of the composition of the spent fuel on the system self-multiplication factor. The critical experiments described here directly address this issue. The objective here is to provide benchmark data to verify the accuracy of the methods used to determine the criticality safety of spent nuclear fuel shipping, storage, and disposal configurations.

The ability to accurately predict the multiplication factor for spent nuclear fuel configurations depends on two important factors: (1) accurate determination of the constituents of the spent fuel, and (2) accurate calculation of the multiplication factor for the known composition and geometry. The experiments reported here provide benchmark data for critical systems with accurately known composition in a geometry that is easily modeled with the current generation of criticality safety analysis software. This research produced criticality data specifically applicable to transportation and storage of spent nuclear fuel and provides a general experimental configuration and capability that can be further used to augment the existing criticality database.

3.2. Project Justification

A large amount of time, money, and effort are to be invested in the storage, transportation and disposal of spent nuclear fuel (SNF). A significant fraction of the costs is proportional to the number of containers required for the storage, transportation and disposal of SNF. Currently, the number of canisters required is conservatively high as a result of numerous conservative assumptions in the safety analyses required by regulators. These conservative assumptions are required because of the paucity of criticality safety benchmarks that include fission product isotopes in the neutron spectra associated with storage, transportation and disposal environments of SNF.

The DOE Office of Civilian Radioactive Waste Management (OCRWM) has been particularly concerned with minimization of shipments to a geologic repository and therefore with maximizing the quantity of SNF within transportation packages. The primary emphasis in this effort has been to obtain burnup credit, that is, credit for the isotopic changes in the fuel during its burnup history. It has been proposed that burnup credit can produce significant national budget savings in reduced transportation costs alone. This effort to obtain burnup credit has met with significant resistance from the Nuclear Regulatory

Commission (NRC). That resistance was based on the uncertainty of the calculated isotopics resulting from fuel burnup and on the uncertainty in the nuclear data for fission products used in the criticality analyses.

The resistance in the area of burnup credit resulted in OCRWM taking a tiered approach in applying for acceptance by the Nuclear Regulatory Commission. DOE OCRWM submitted the Actinide-Only Burnup Credit Topical Report (DOE 1998) to the NRC for approval. In response, the NRC issued Interim Staff Guidance on burnup credit (NRC 1999) that allowed the use of actinide-only burnup credit. The restriction to just actinides provides only a fraction of the desired level of criticality burnup credit. The need for the restriction illuminates the general need for additional criticality data. Furthermore, it points to regulatory issues about integral benchmarks. Specifically, it indicates that regulators are unwilling to accept small errors that may be due to a cancellation of two or more competing errors. In order to address this regulatory concern it is essential that the isotopics calculations (calculations that track the material composition changes that are a result of burnup) and the criticality calculations be benchmarked separately. This logic can be extended to fission product constituents, that is, that the effect of each constituent that affects the reactivity of a system be benchmarked separately for its effect on the calculation.

This project addresses the issue of criticality calculations in systems containing fission products. It provides new benchmark data on rhodium, one of the important fission product absorbers. These results, coupled with the results of follow-on experiments that investigate other fission products, can be used to quantify and reduce the conservatism of the SNF safety analyses while still providing the necessary level of safety.

3.3. Earlier Work

This experiment is similar to one that was proposed earlier at Sandia (Harms 1995). The Spent Fuel Safety Experiment (SFSX) was a critical experiment designed to measure the integral worth of spent fuel. The SFSX was designed but not completed. The SFSX was a fuel-replacement experiment. As such, it consisted of a series of three approach-to-critical experiments. The first experiment was to use only fresh “driver” fuel elements and provide the first benchmark in the series and a demonstration of the approach to critical procedures. The primary benefit of this fresh fuel data point was to provide a benchmark in a very “clean” configuration. It also would provide a basis for the determination of the spent fuel worth, which was to be measured in subsequent approach-to-critical experiments.

For the second experiment, the seven centrally located driver fuel elements were to be replaced by spent fuel taken from the midsection of a spent-fuel assembly that had been chemically analyzed earlier. The center sections of the spent fuel rods were selected specifically to eliminate considerations of axial burnup variations. Replacing the fresh fuel with the spent fuel would have resulted in a decrease in multiplication, directly providing the reactivity worth of the spent fuel. Fresh fuel was to be added to the remaining outer locations in the assembly until a delayed critical configuration was reached. This configuration was the benchmark data point for calculation of a spent fuel critical.

The third experiment was similar to the second except that the spent fuel was to have originated from the end sections of the spent fuel assembly. The distribution of burnup effects, particularly the under-burned ends of the fuel rods, was addressed by this third

measurement. Because the burnup of the end fuel section had a strong gradient, this measurement, in addition to giving a comparison of the worth of end and center sections, provided a challenging benchmark for axial nodalization in criticality calculations.

A sketch of the SFSX assembly is shown in Figure 3-1. The assembly was designed to provide "clean" criticals in which the only materials that had a significant effect on the reactivity of the system (the driver fuel, the irradiated fuel sample, and the water moderator) were well characterized. The assembly had fuel-followed control and safety rods which, when fully raised, were neutronically identical to driver fuel rods. The assembly was designed so that the spent fuel could be lowered from the assembly into a well-shielded position below the floor level of the reactor room.

The driver fuel for the SFSX was 4.31 % enriched UO_2 pellets with an outside diameter of 1.27 cm. This fuel was fabricated with a nominal 50-cm fuel height. The cladding was Zircaloy-4 with a 1.27-cm-thick lower end plug and a 2.54-cm-thick upper end plug. The

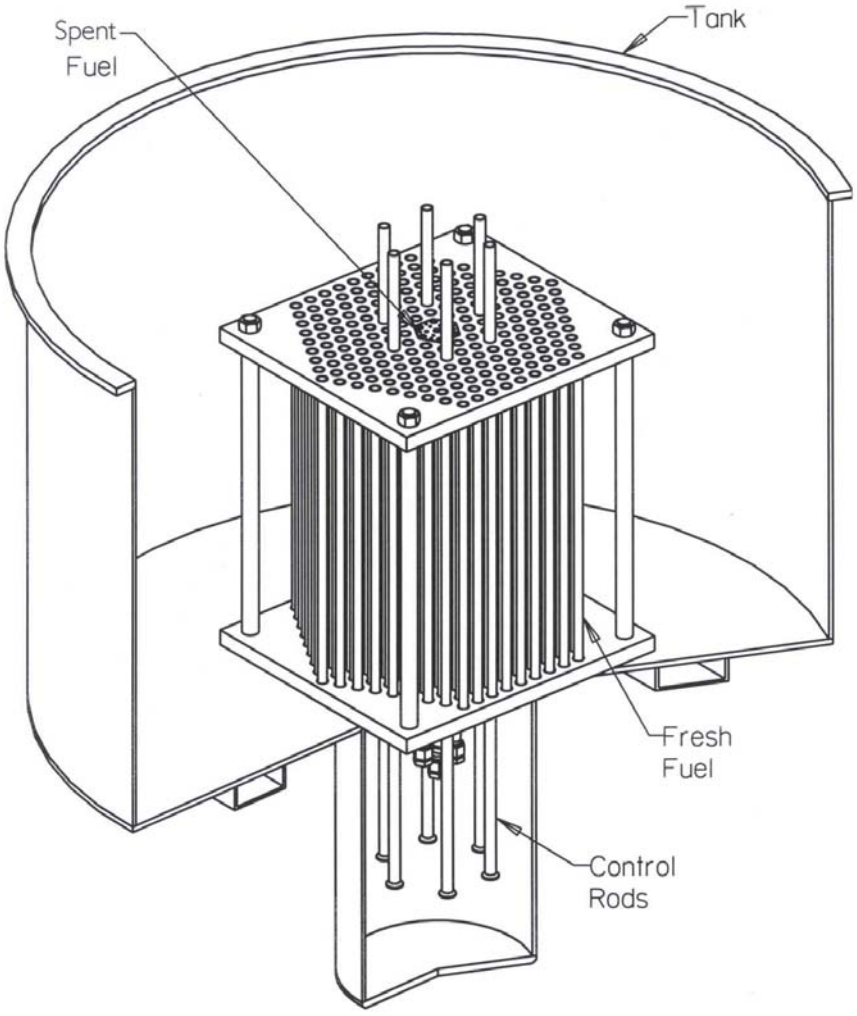

Figure 3-1. **Sketch of the Spent Fuel Safety Experiment critical assembly.**

assembly and the driver fuel rods were designed such that when the fuel was inserted in the assembly, the top of the lower end plug was at the elevation of the top of the lower grid plate. The upper and lower edges of the upper end plug were at the same elevations as the upper and lower surfaces of the upper grid plate. As a result, the end plugs in the fresh fuel exactly filled the holes drilled in the grid plates. The assembly could be modeled as a fuel/clad/water region with solid metal plates above and below surrounded by a water reflector.

The SFSX assembly was designed for optimum sensitivity to the effects of interest rather than to mock up any specific fuel configuration. The fuel rod pitch was chosen to minimize the total fuel loading at delayed critical (DC). The fuel height was set at 50 cm to give adequate sensitivity to the burnup gradients that exist over a relatively short distance at the ends of spent fuel rods.

The SFSX was funded by the OCRWM. The SFSX was designed, but the experiment was not completed. However, several aspects of the SFSX project benefited this project. First, the driver fuel for the SFSX was fabricated and available to this project. Second, the Authorization Basis (AB) for the SFSX had been partially established and was used as the basis for the AB for this project. Finally, the design concept of the current experiment is very similar to the SFSX design concept.

4. Overview of the Project

The project, as envisioned in the original proposal, involved five major tasks. The five tasks are described below.

4.1. Task 1: Obtain the Required NEPA Approvals

This task involved assuring compliance of the project with the NEPA. An Environmental Checklist was filed with the Department of Energy requesting that the project be categorically excluded from further NEPA documentation based on the fact that it was an activity similar to that which had been carried out in the facility for many years. The DOE granted the request. This task consumed a relatively small fraction of the project resources.

4.2. Task 2: Obtain Safety Basis Approvals

In order to operate the critical experiment in the SPRF, the experiment activities were required to be enveloped by the approved authorization basis (AB) for the SPRF. The Sandia Pulsed Reactor III (SPR-III) is an unmoderated fully-enriched metal-fueled fast burst reactor. The experiment uses a water-moderated array of UO_2 fuel rods in the critical assembly. Though the hazards of the pulsed reactor enveloped the hazards presented by the critical experiment, the requirements for the two were significantly different.

To address the difference between the SPR-III characteristics and those of the critical experiment, an addendum to the SPRF SAR (SNL 2002a) was written that described the characteristics and hazards of the critical experiment. Chapters were written that covered the critical assembly, the critical assembly control system, and the potential hazards and accidents associated with the experiment. An attempt was made to write the SAR addendum generally enough that a range of experiments could be done within the envelope described. The attempt was successful because a second critical experiment, this one with different fuel and different goals from the BUCCX, was funded in 2001 as NERI project 01-124 and was in progress when this report was written.

The TSRs for the critical experiment (SNL 2002b) record the actions and conditions necessary to operate the critical experiments within the safety envelope defined in the SAR addendum. The two documents represent a basis to safely operate a range of critical experiments in the SPRF.

After the SAR addendum and the TSRs were completed, these were submitted to a three-level independent review process. The first level of review occurred in the Sandia Pulsed Reactor Committee (SPRC), a committee of engineers, scientists, and reactor operators from the reactor facility with working expertise in the operational safety of nuclear reactors. In this review, the documents received a thorough line-by-line scrubbing. The next level of review came from the Sandia Nuclear Facilities Safety Committee, a committee of individuals from both inside Sandia and outside Sandia with broad expertise in nuclear facility safety. The documents received a higher-level but still thorough review. Finally, the documents were submitted to the DOE for review and approval. Approval was granted.

The AB documents were reviewed for areas requiring formalization in operating procedures. Seventeen formal Safe Operating Procedures and Technical Work Documents were written to control various aspects of the work.

A Readiness Assessment (RA) was required before experiment operations commenced. The intent of the RA was to assure Sandia and DOE that Sandia was prepared to operate the critical experiments safely. The RA consisted of three parts: a management self-assessment by the reactor operations group, a Sandia RA by a Sandia group independent of the operations group, and a DOE RA. All findings of the three parts were closed out prior to operations.

The safety basis work was envisioned in the proposal as a significant task but not one that dominated the project. As the project evolved, this work consumed a large fraction of the available resources.

4.3. Task 3: Design and Procure the Critical Assembly Hardware

This task included the design and fabrication of the hardware used in the critical assembly. This critical experiment benefited from the hardware built for earlier critical experiments. The critical assembly hardware was based on the hardware used for a critical experiment conducted for the Space Nuclear Thermal Propulsion (SNTP) program (SNL 1989). The driver fuel was built for the Spent Fuel Safety Experiment (Harms 1995) and used fuel material from the Critical Mass Laboratory at the Pacific Northwest National Laboratory.

The nuclear and mechanical design of the critical experiment hardware was performed as part of this task. Though the design was based on the earlier SNTP experiment, differences in the fuel required that much of the core hardware be redesigned. Once the hardware was designed, it was put out for bid. The new hardware was fabricated and delivered to Sandia.

The control requirements for this experiment were similar to those for the SNTP critical experiment. The instrument and control system from the earlier SNTP experiment was modified slightly and refurbished for use with the present experiment.

Driver fuel elements had been fabricated for an earlier critical experiment (Harms 1995) using excess low-enriched UO_2 fuel material from the Critical Mass Laboratory at the Pacific Northwest National Laboratory. The fuel, which had originally been clad in aluminum, was reclad into Zircaloy-4 by a commercial nuclear fuel manufacturer as part of the SFSX project. The 350 fuel elements had been stored at Los Alamos National Laboratory after fabrication and were shipped to Sandia for use in this experiment.

The driver fuel elements contain a large fraction of the fuel in the critical experiments. Special fuel elements were required for control/safety elements, a source element, and experiment fuel elements. The remainder of the stock of fuel that was used in fabricating the driver fuel elements was obtained from the Pacific Northwest National Laboratory. This fuel was sent to the same firm that built the driver fuel elements and the UO_2 fuel pellets were removed from the aluminum cladding. The same company fabricated Zircaloy-4 tubes that were used for the control/safety elements, source element, and experiment elements. The pellets and tubes were sent to Sandia where the fuel and other element internals were loaded into the tubes and the tubes were sealed.

This task was envisioned in the proposal as a straightforward process of the design, procurement and construction of the experiment fuel and hardware. Significant obstacles were surmounted, with the help of DOE NE-20 to move the fabrication of the special fuel elements forward. The remainder of the work under this task went as anticipated.

4.4. Task 4: Perform the Critical Experiments

This task included the design and execution of the critical experiments. A basic part of the experiment design was selection of the experiment philosophy and of the materials to be tested. To accomplish this, an ad hoc panel of burnup credit experts was gathered together to advise the experiment team. The panel made two recommendations: 1) do a few critical experiments well rather than many experiments in less depth, and 2) use rhodium as the first test material. Both recommendations were accepted.

The experiment design called for the placement of foils of a test material between the fuel pellets in the experiment fuel elements. The test material selected was rhodium. Thirty-one foils were required to place a foil between the 32 fuel pellets in each experiment fuel element. Because each experiment contains 36 experiment fuel elements loaded with foils, 1116 foils were required per experiment. Three sets of 1200 rhodium foils were obtained at nominal thicknesses of 0.025, 0.05 and 0.1 mm. The purity of the rhodium was 99.9%. The rhodium foils were loaded into three sets of experiment fuel elements.

Ten critical experiments, detailed below, were performed during the project.

4.5. Task 5: Decontaminate and Decommission the Assembly

Under this task, the critical experiment hardware was removed from service, cleaned, and stored for future use. The driver fuel was stored in 55-gallon 6M containers and transported to a storage location. The experiment fuel elements, control/safety fuel elements, and source fuel element were stored at the reactor facility that hosted the critical experiments. The critical assembly hardware was moved to a storage location. All of the experiment hardware is easily retrievable so that it can be readily used for future critical experiments.

5. Critical Assembly Design

The overall concept of the critical assembly is shown in Figure 5-1. The assembly core resides in an elevated assembly tank that is connected to a moderator dump tank at a lower elevation. When the assembly is not being operated, the moderator resides in the dump tank.

When the assembly is being brought to critical, the moderator is pumped from the dump tank into the assembly tank. The moderator is released by gravity to the dump tank through two large-diameter pneumatically operated dump valves. A heater is included in the dump tank to keep the moderator at a constant temperature set by a controller at the assembly control system. During operation, the moderator is continually circulated between the dump tank and the assembly tank. The level of the moderator in the assembly tank is set by a standpipe.

The assembly fuel is supported in the assembly tank by two 2.54 cm (1 in) thick aluminum grid plates. The grid plates are located in the tank to provide a 15.24 cm (6 in) thick water reflector below the lower grid plate. The diameter of the tank provides a radial water reflector around the assembly greater than 15.24 cm. The assembly tank standpipe is set to provide a 15.24 cm (6 in) thick upper reflector when the assembly tank is full.

The assembly has one control and two safety elements of identical design. The two types of elements are differentiated by the way in which they are used. During operations, the two safety elements are held in the most reactive position and provide a redundant shutdown mechanism that can be rapidly inserted by gravity drop. The control element is used to make fine adjustments to the reactivity of the assembly during operations. The three control/safety elements are attached to the SNTP CX control rod drives through electromagnets. The control element drives are supported above the assembly tank by the drive support.

5.1. Fuel

5.1.1. Driver Fuel Elements

Most of the fuel elements in any given critical array were driver fuel elements. The design of the driver fuel elements is shown in Figure 5-2. The driver fuel elements were fabricated in 1996 by Siemens Power Corporation from UO_2 fuel pellets supplied by the Pacific Northwest National Laboratory (PNNL) using Zircaloy-4 tubing welded to end plugs of Zircaloy-2 or Zircaloy-4.

The UO_2 fuel pellets in the fuel elements were in fuel rods used in critical experiments at the Critical Mass Laboratory at the PNNL. Several of the experiments are documented in the International Handbook of Evaluated Criticality Experiments (NEA 2001) as LEU-COMP-THERM-002 and others. According to the documentation of those experiments, the uranium is 4.306 percent enriched and has a density of 10.4 g/cm^3. The outside diameter of the fuel pellets is 1.265 ± 0.003 cm (0.498 ± 0.001 in). The nominal stack height of the UO_2 pellets is 49.213 cm (19.375 in). According to the material accountability records, mass of the UO_2 in the fuel rods was measured to the nearest half gram and ranged from a minimum of 616 g to a maximum of 652 g with an average of 637.73 g. The average ^{235}U content of the driver elements is 24.12 g with a maximum of 24.66 g and a minimum of 23.32 g.

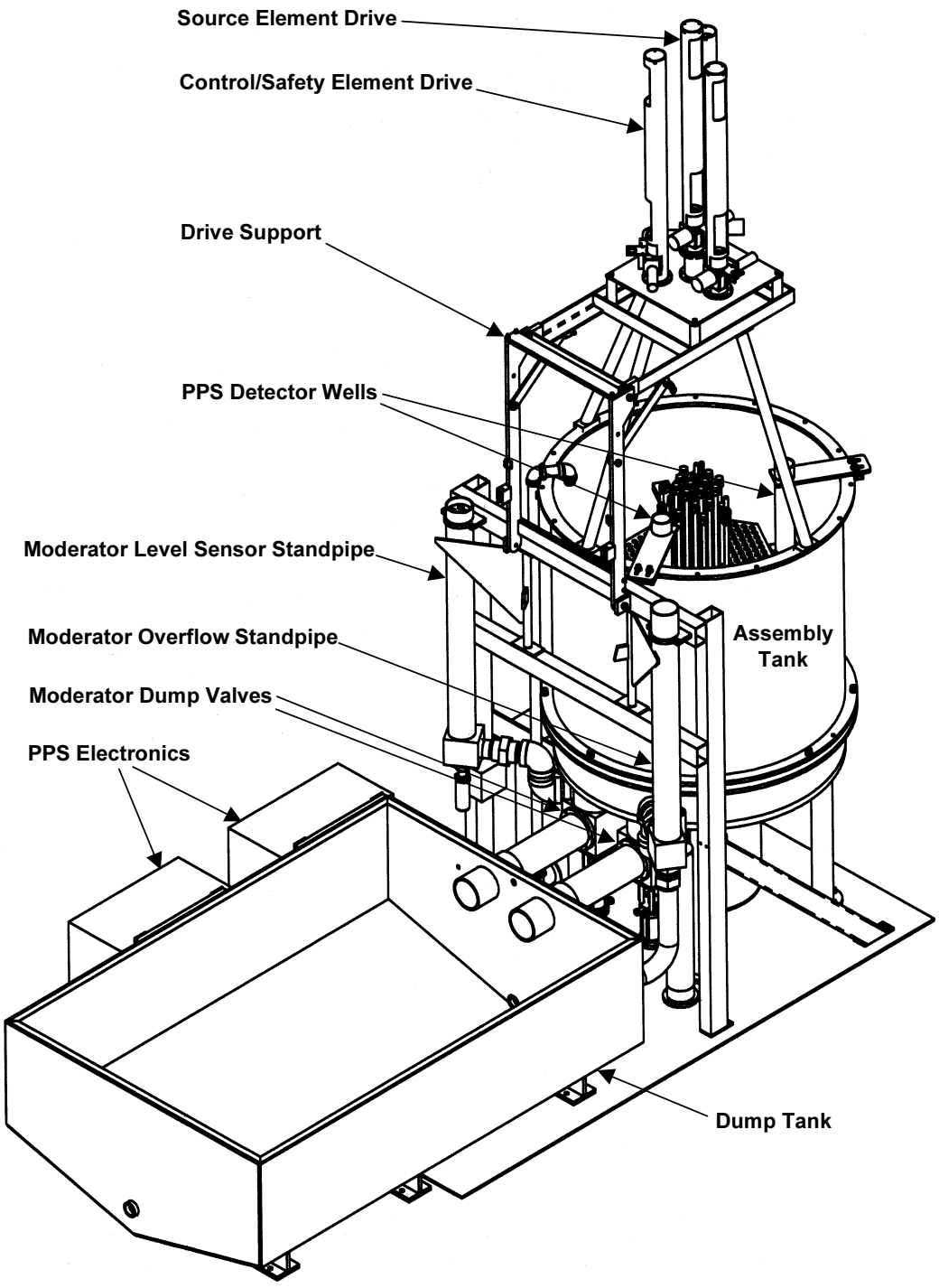

Figure 5-1. Overall view of the BUCCX critical assembly.

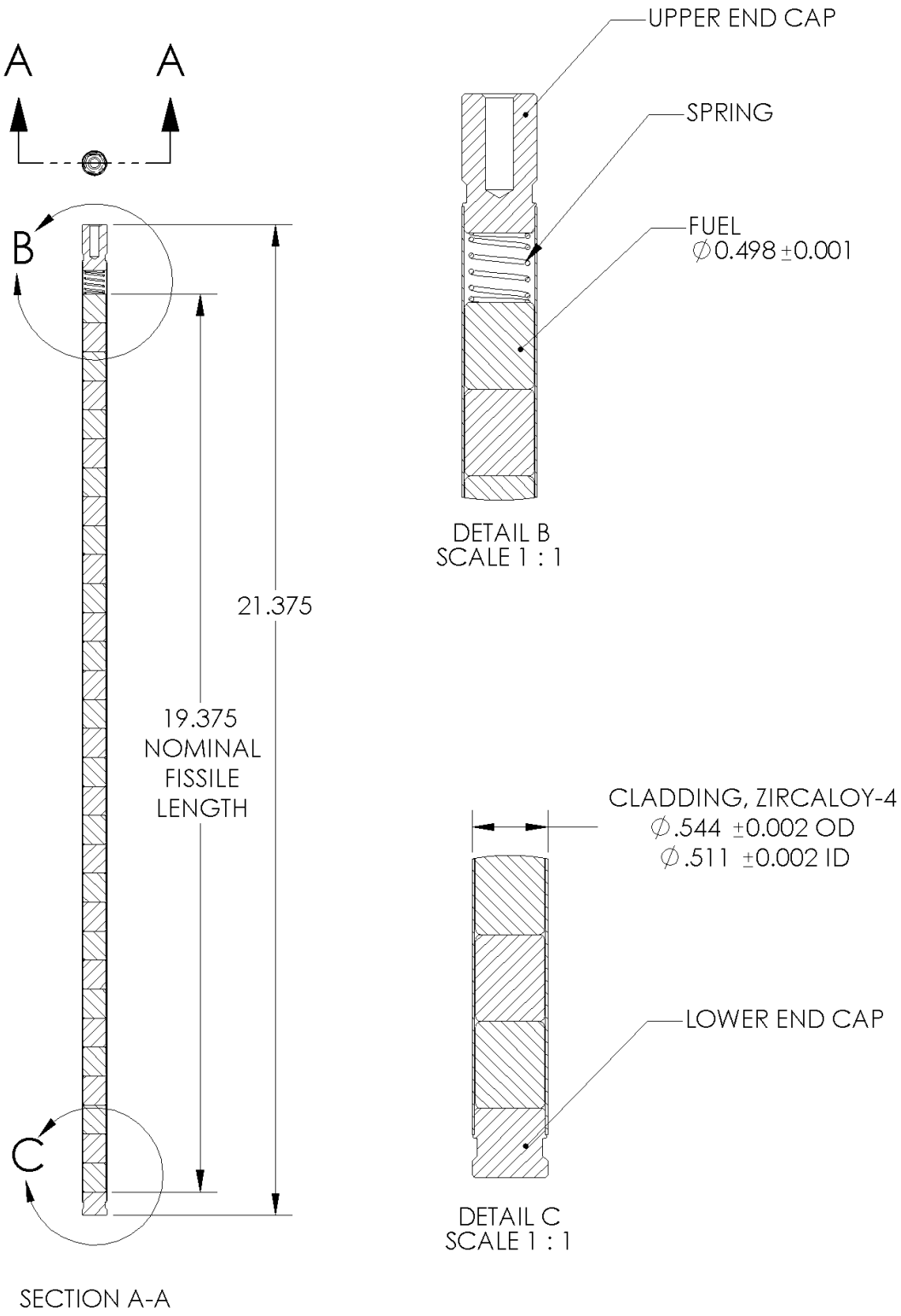

Figure 5-2. Details of the driver fuel element design. The dimensions are given in inches.

The cladding tubes were fabricated from Zircaloy-4 instrument or guide tubes with an outer diameter of 1.382 ± 0.005 cm (0.544 ± 0.002 in) and an inner diameter of 1.298 ± 0.005 cm (0.511± 0.002 in) giving a nominal wall thickness or 0.042 cm (0.017 in). The fuel elements were sealed at the bottom by welding to a 1.27 cm (0.5 in) end plug of Zircaloy-2 or Zircaloy-4. The top is sealed by welding the tube to a 2.54 cm (1 in) plug of the same material. Both end plugs incorporated a circumferential groove. The top plugs had a threaded hole for use with a handling fixture. A corrosion-resistant spring was placed between the fuel pellets and the top plug. Before the final seal weld was made, the elements were pressurized with helium. After the final seal weld, a helium leak check was made to verify that the leak rate was less than $1x10^{-8}$ cc/s of helium.

The driver fuel elements were designed to be supported by two 2.54 cm (1 in) thick grid plates. The bottom plug fits in a 1.27 cm (0.5 in) deep hole in the lower grid plate. The lower plug then lines up with the grid plate to make the combination appear as a solid sheet of metal. With the appropriate grid plate spacing, the upper plug of the fuel elements lines up with the upper grid plate, making the upper plug/grid plate to appear neutronically as a solid sheet of metal.

5.1.2. Experiment Fuel Elements

The experiment fuel elements are designed to mimic the driver fuel elements neutronically while allowing access to the fuel pellets in the element so that experiment materials can be placed between the fuel pellets.

The cladding tubes for the experiment fuel elements have the same radial dimensions as the tubes for the driver fuel elements but are longer. The bottom plugs for the experiment fuel elements are identical to those for the driver fuel elements. The upper end of the experiment fuel elements is sealed by a 14 mm Swagelok cap. The experiment elements are longer than driver elements so that the cap is well away from the assembly fuel and will not affect the experiment results. Between the bottom plug and the cap, the materials inside the clad tube stack up as follows: 1) fuel pellets from the same source as the driver fuel elements with the same nominal stack height; 2) corrosion resistant spring; 3) 2.54 cm (1 inch) tall Zircaloy-2 or Zircaloy-4 plug to line up with the upper grid plate; and 4) polyethylene plug.

The experiment elements were made in three lengths so that the caps can be staggered in experiments where the fuel element pitch will not allow the caps to be placed side by side. In all experiment elements, the fuel pellet stack, spring, and Zircaloy plug were the same height. Polyethylene plugs of different lengths make up the differences in element length. The diameter of the polyethylene plugs was set so that the hydrogen in the polyethylene exactly replaces the hydrogen in the water displaced by the fuel rod.

Experiment materials can be placed between the fuel pellets in the experiment elements. In the critical experiments described here, rhodium foils with the same diameter as the fuel pellets were placed between the fuel pellets in the experiment elements.

5.1.3. Control and Safety Elements

The critical assembly has three identical fuel-followed control/safety elements, two operated as safety elements and one operated as a control element. During the execution of a critical experiment, the safety elements are held at their most reactive position. In this position, the safety elements provide a large negative reactivity that is available to quickly shut down the assembly should the need arise. The absorber section in the elements is also well away from the assembly core and does not affect the reactivity of the system. The control element is used during critical assembly operations to make fine adjustments in the reactivity of the assembly.

The fueled section of the control/safety elements is similar to an experiment element. In order to allow the elements to be lowered from the assembly, the lower grid plate has through holes at the control/safety element positions. To fill the grid plate hole completely, the bottom plugs on the control/safety elements are 2.54 cm (1 in) long. The bottom plugs are the same design as the top plugs used in the driver fuel elements. Above the bottom plug, the materials stack up the same as the materials in the experiment elements with the inclusion above the polyethylene plug of an absorber section and another polyethylene plug. The upper seal of the control/safety element is made by a Swagelok union that couples the element to a threaded stainless steel fixture used to connect the element to the element drive through an electromagnet.

The absorber section in the control/safety elements is an aluminum tube 1.27 cm (0.5 in) OD with 0.071 cm (0.028 in) walls plugged at both ends with 0.965 cm (0.38 in) aluminum plugs. Inside the tube are eleven sintered natural B_4C pellets, 5.08 cm (2.00 in) long by 1.102 cm (0.434 in) diameter, with a nominal stack height of 55.88 cm (22 in). The average mass of the B_4C in the absorber sections is 96.88 g. The B_4C pellets are held at the bottom of the absorber section by a corrosion resistant spring.

5.1.4. Source Element

The source fuel element is a double fuel element with the two fueled sections separated by a 15.24 cm (6 in) polyethylene plug. The source element is attached to a drive similar to the control/safety element drives except that the source element is solidly attached to the drive without an electromagnet. The upper fueled section mimics a driver fuel element. The lower fueled section is similar to a driver fuel element except that the central three fuel pellets are replaced by a sealed ^{252}Cf neutron source. The lengths of the elements in the source rod are set so the Zircaloy plugs in the lower section line up with the grid plates when the source element is “up” and the same is true of the Zircaloy plugs in the upper section when the element is “down.” The neutron source was used to drive the critical assembly during approach-to-critical experiments. Once a self-sustaining chain reaction was established, the neutron source element was lowered from the assembly replacing the fueled section containing the source with a fueled section with no source.

The neutron source is a commercially available source containing ^{252}Cf. The source was manufactured by Isotope Products Laboratory (IPL) and was listed in the IPL catalog as “Capsule 3014.” The source was inserted into a holder fabricated from aluminum that had an overall length of 3.195 cm (1.258 in). The bottom of the source holder was 21.695 cm (8.541 in) above the bottom of the fuel. The arrangement of the source in the source holder

is shown in Figure 5-3. The inset of the figure shows a diagram of the stainless steel 304 source capsule from the IPL catalog.

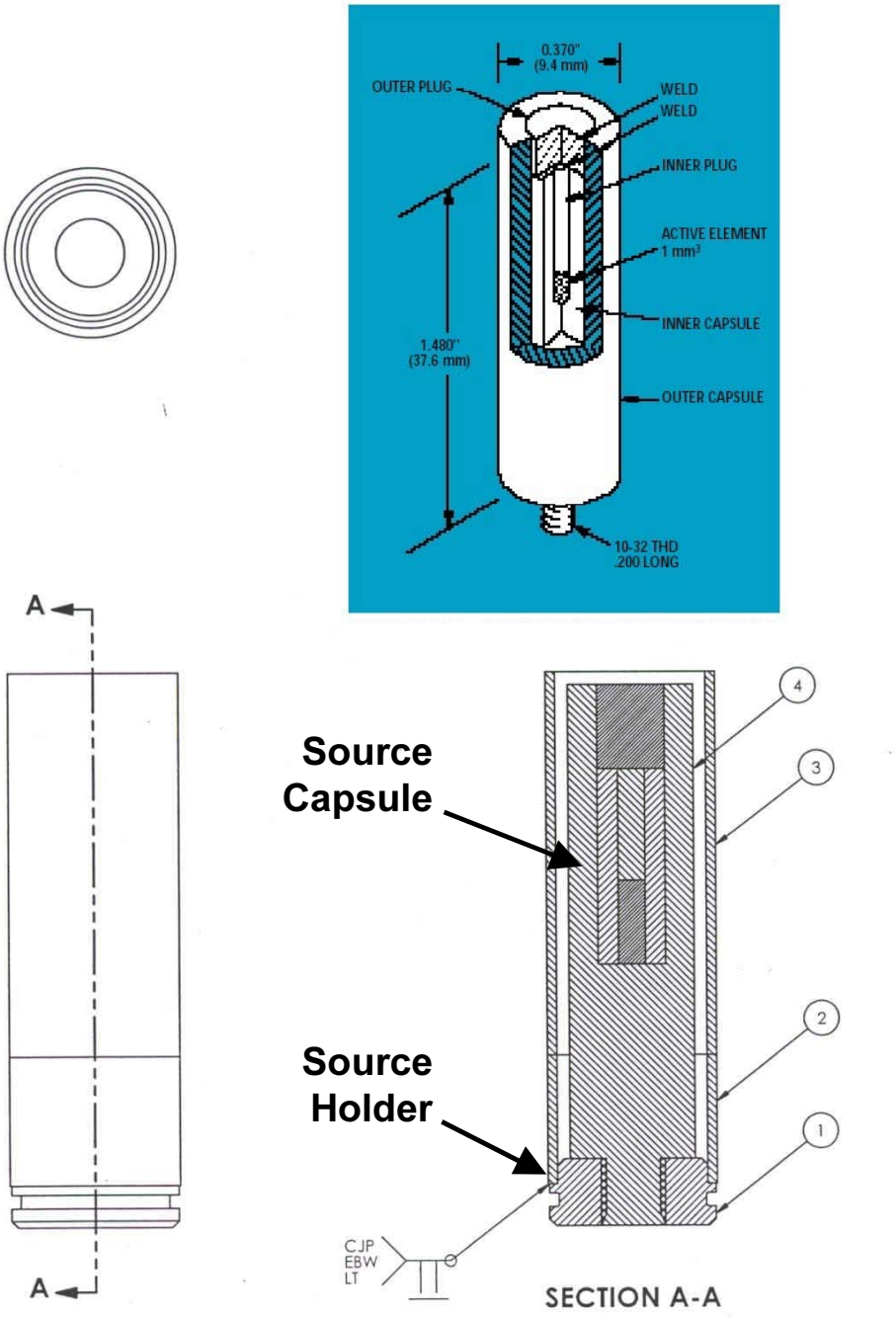

Figure 5-3. The neutron source and holder. The inset is a figure from the IPL catalog showing the geometry of the neutron source capsule.

5.2. Hardware

5.2.1. Grid Plates

The two aluminum grid plates support and maintain the spacing of the fuel elements in the critical assembly. Both grid plates are 2.54 cm (1 in) thick. The lower grid plate is circular and is supported by a ring that is part of the assembly tank. The lower grid plate has six large holes in it to allow passage of the moderator when the dump valves are opened. The upper grid plate is hexagonal with three support bosses 120 degrees apart. The holes for the fuel elements in the upper grid plate are numbered for identification. The upper grid plate is supported from the lower grid plate by three threaded aluminum standoffs.

The lower grid plate has 1.27 cm (0.5 in) deep holes bored in it to support and locate the bottom of the fuel elements. The upper grid plate has matching through holes in it to locate the top of the fuel elements. The central hole and three holes spaced 120 degrees apart are bored through in both grid plates to a slightly larger diameter to allow the source and control/safety elements to freely move through the grid plates.

Two sets of grid plates were fabricated, one with the holes on a 2.8 cm triangular pitch and one with the holes on a 2.0 cm triangular pitch. The fuel elements in the experiment, when placed in a 2.0 cm triangular pitch, have a fuel-to-water ratio similar to that of a pressurized water reactor fuel assembly. With a 2.8 cm pitch, the fuel elements are nearly optimally moderated.

5.2.2. Assembly Tank

The assembly tank supports the assembly and contains the moderator during approach-to-critical experiments. The dimensions of the assembly tank are such that the assembly has 15.24 cm (6 in) thick top and bottom reflectors and at least the same thickness radial reflector when the tank is full of moderator. The tank is essentially cylindrical with a cylindrical projection out the bottom to accommodate the motion of the source and control/safety elements. The assembly tank consists of two weldments and the grid plate support ring.

The lower tank weldment has a 2.54 cm (1 in) thick floor that provides support for the assembly tank. The floor is drilled and tapped to accommodate the tank supports and has holes to connect to the two moderator dump valves. The floor also has a large central hole for the projection. The weldment has a flange at the top with an O-ring groove used for connection to the grid plate support ring.

The upper tank weldment is essentially a flanged tube. The lower flange is drilled to match the flange on the lower tank weldment and the grid plate support ring. The upper flange is drilled to connect to the support structure for the control/safety and source element drives. The inside diameter of the tank is 93.68 cm (36.88 in).

The grid plate support ring fits between the upper and lower tank weldments and has an O-ring groove in the surface that mates with the lower flange on the upper tank weldment. The lower grid plate attaches to the grid plate support ring.

The assembly tank is connected to two standpipes. One standpipe contains a linear moderator level sensor. The other contains an overflow pipe that determines the moderator

level. The assembly tank also has a float switch used to indicate that the tank is full of moderator.

5.2.3. Moderator Handling System

The dump tank is a large vessel that is at a lower elevation than the assembly tank. The two tanks are connected through two large-diameter pneumatically-operated normally-open dump valves. When the assembly is shut down or fuel is being loaded during an experiment, the dump valves are open and the moderator is in the dump tank. To make a multiplication measurement, the following sequence of events occurs:

1. The dump valves are closed.
2. Moderator is pumped from the dump tank to the assembly tank with the "fast" fill pump. It takes about 15 minutes to fill the assembly tank in this mode.
3. When the float switch indicates "full," the "fast" fill pump is turned off and a smaller recirculating pump is turned on. The recirculating pump fills the assembly tank to the overflow standpipe and continues circulating water between the dump tank and the assembly tank to prevent thermal stratification of the moderator in the assembly tank. This also ensures that the moderator level is constant from measurement to measurement.
4. At the end of the measurement, the dump valves are opened and the moderator flows from the assembly tank to the dump tank.

The dump tank has an electrically-operated heater that is used to maintain a constant moderator temperature. The heater can be used to elevate the moderator temperature several degrees to explore the effect of temperature on the critical assembly.

5.2.4. Instrumentation and Control System

The Instrument and Control (I&C) system for the assembly is divided into two subsystems: (1) The Plant Protection System (PPS), which provides the automatic scram function of the I&C system, and (2) the control system, which includes the equipment necessary for remote manipulation of all reactivity control mechanisms, startup source, and monitoring equipment. The automatic scram function refers to the automatic trip of the PPS to shutdown the assembly and protect the fuel elements.

5.2.4.1. Plant Protection System

The function of the Plant Protection System (PPS) is to rapidly scram the critical assembly if power level or period exceeds prescribed limits. The protection system is made up of two redundant channels of neutron flux monitoring systems and the magnet power supply trip system. A trip signal from either channel causes a scram independently of the other channel. There are also manual scrams operable from the control console and the reactor building.

The neutron flux monitor consists of a neutron detector, an amplifier assembly, and a signal processor. The neutron detectors are fission chambers that are placed in the detector wells in the assembly tank. The locations of the detector wells are adjusted to give an appropriate count-rate range to cover the operating conditions of the assembly. The amplifier assembly houses the power supplies and the electronics that condition the detector signal for

transmission to the signal processor. The signal conditioning electronics in the amplifier assembly provide amplification, pulse shaping, and discrimination against alpha and gamma radiation and electronic noise, and other signal conditioning to provide an output signal that can be transmitted over a twisted-shielded pair. The signal processor converts the signal from the amplifier into signals that represent the source range count rate, the power level, and the rate of change of power level (period), and provides trip signals to the magnet power supply when any signal is outside a predetermined set point.

5.2.4.2. Control System

The control system portion of the Instrumentation and Control (I&C) system provides essential data to the operator for safe operation of the critical assembly, including core tank temperature, core tank level, control/safety element position and source position. The control panel is the means of remotely controlling reactivity addition or withdrawal from the core when the assembly is at or near delayed critical.

The position of each of the control and safety elements is indicated by a digital meter that uses a bridge type circuit with a position potentiometer in one leg of the circuit. Control and safety element drive full-in and full-out positions are displayed using indicating lamps controlled by limit switches located on the element drive package. Additional lamps and limit switches provide indication when the element is fully down (seated) and when it is coupled to the drive mechanism. Only the "up" (fully-out) indication is required for operation.

5.2.4.3. Count-Rate Instrumentation

The count-rate instrumentation is used during an approach-to-critical experiment to measure the assembly multiplication. For all the critical experiments, the count-rate instrumentation included two scaler-timers, each counting pulses on buffered outputs from the two PPS channels. A third channel was added for several of the critical experiments. This channel was independent of the PPS and consisted of a fission chamber, preamplifier, amplifier, single channel analyzer, and scaler-timer. The detector for this channel was outside but immediately adjacent to the assembly tank.

6. The Experiments

6.1. Approach-to-Critical Experiments

The critical experiments were done using the classical inverse multiplication method to do an approach-to-critical experiment. The multiplication M of an assembly of fissile material is given by

$$M = \frac{k_{eff}}{1 - k_{eff}}$$

where k_{eff} is the eigenvalue of the fissile material. When the assembly subcritical, k_{eff} is less than 1 and the multiplication is finite. When the assembly is exactly critical, k_{eff} is 1 and the multiplication is infinite. The inverse of the multiplication is positive when the assembly is subcritical and zero when the assembly is critical.

During an approach-to-critical experiment, the assembly is driven by a constant neutron source. For the experiments reported here, the neutron source was a small capsule containing ^{252}Cf that emitted about 10^7 neutrons per second. Given a constant source, the neutron population in the assembly is proportional to the multiplication of the assembly. A neutron detector placed in or near the assembly will respond to the neutron population at the detector location and will therefore give an indication that is proportional to the assembly multiplication.

An approach-to-critical experiment is done by making a series of multiplication measurements as a function of increasing reactivity in the assembly. The parameter that increases the assembly reactivity can be one of many choices. In the case of the experiments reported here, the approach was made by varying the amount of fuel in the assembly. The recipe for the approach-to-critical experiments done in this project is as follows:

1. To start the experiment, detector readings are taken with an array that has been shown by calculation to be subcritical. Fuel is added to the assembly to reach a more reactive configuration that has also been shown by calculation to be subcritical. Detector readings are again taken.
2. The inverse of the detector readings is plotted against the number of fuel elements in the assembly. A straight-line projection is made between the two points to an inverse detector reading (inverse multiplication) of zero. At this point, the number of fuel rods that are projected to produce an inverse multiplication of zero is the current estimate of the critical array size.
3. From this point, the additions of fuel are guided by the measurements of the multiplication of the assembly. The difference between the current estimate of the critical array size and the array size at the last measurement is divided by two and rounded down to the nearest integer to get the number of fuel elements to be added to the assembly for the next reactivity step.

4. After the fuel element increment is added to the assembly, a new multiplication measurement is made. A linear extrapolation of the new inverse multiplication and the one immediately preceding it to zero gives a new estimate of the critical array size.
5. The preceding two steps are repeated until the fuel element increment falls below one fuel element.
6. The experiment is then walked upward in reactivity in one-element increments until a period is measured. Count rate measurements are taken at each fuel increment and plotted to refine the estimate of the critical array size.

Figure 6-1 demonstrates the process described above. During an approach-to-critical experiment, each successive measurement should normally produce a better estimate of the critical array size. Figure 6-2 shows two plots of the results of one of the experiments. The left plot shows the estimated critical array size as a function of the number of elements in the assembly. The horizontal dashed line shows the final estimate of the critical array size. The right plot shows the magnitude of the difference between the final critical array size and the estimated critical array size at each array size step. The difference is a few hundredths of a fuel element at the end of the approach.

6.2. Experiment Suite

Ten critical experiments were conducted in this project. The ten experiments were divided into two sets of five with each set having a different fuel element pitch to give different fuel-to-water ratios. The experiments were loaded as follows:

1. All driver fuel elements, 2.0 cm pitch;
2. 36 experiment fuel elements with no foils, 2.0 cm pitch;
3. 36 experiment fuel elements, each containing 31 25-micron rhodium foils between the 32 fuel pellets in the rods (a total of 1116 foils), 2.0 cm pitch;
4. 36 experiment fuel elements, each containing 31 50-micron rhodium foils between the 32 fuel pellets in the rods, 2.0 cm pitch;
5. 36 experiment fuel elements, each containing 31 100-micron rhodium foils between the 32 fuel pellets in the rods, 2.0 cm pitch;
6. All driver fuel elements, 2.8 cm pitch;
7. 36 experiment fuel elements with no foils, 2.8 cm pitch;
8. 36 experiment fuel elements, each containing 31 25-micron rhodium foils between the 32 fuel pellets in the rods, 2.8 cm pitch;
9. 36 experiment fuel elements, each containing 31 50-micron rhodium foils between the 32 fuel pellets in the rods, 2.8 cm pitch;
10. 36 experiment fuel elements, each containing 31 100-micron rhodium foils between the 32 fuel pellets in the rods, 2.8 cm pitch.

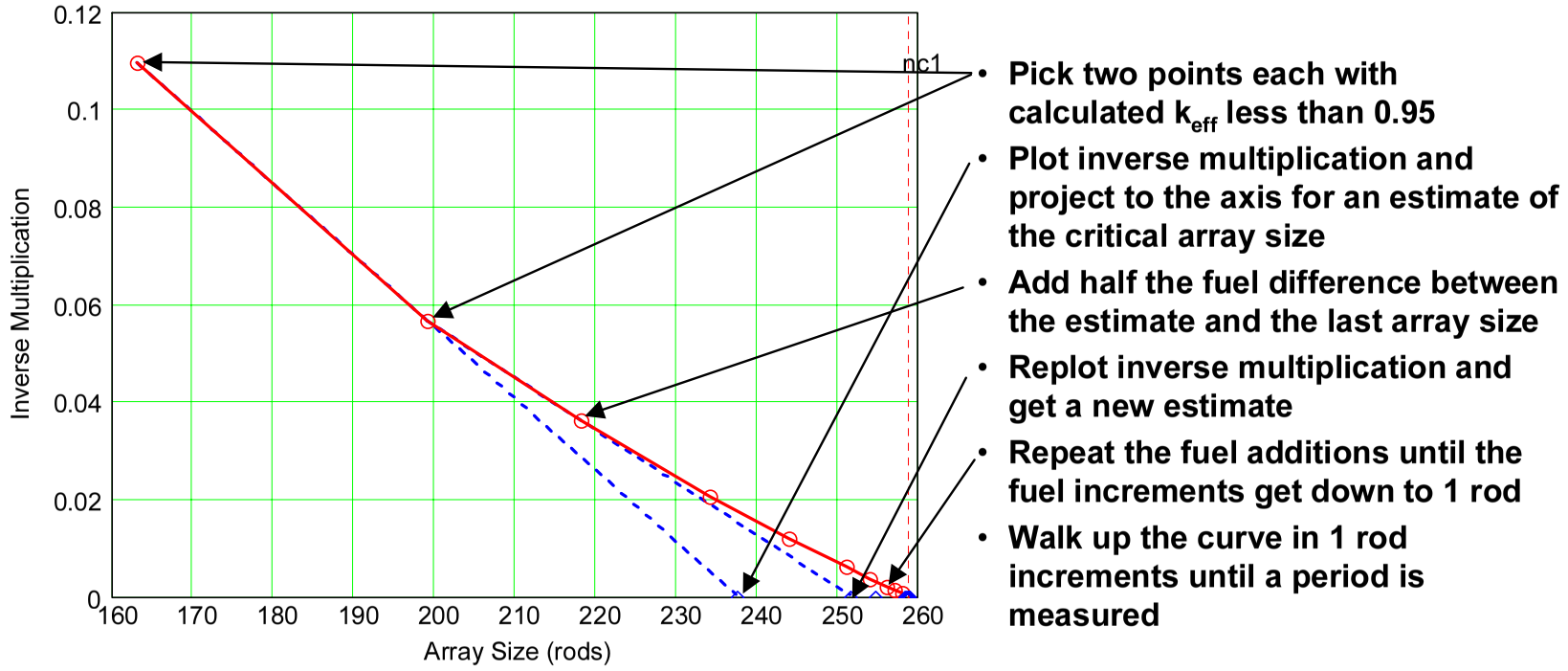

Figure 6-1. Demonstration of the inverse multiplication method for an approach-to-critical experiment.

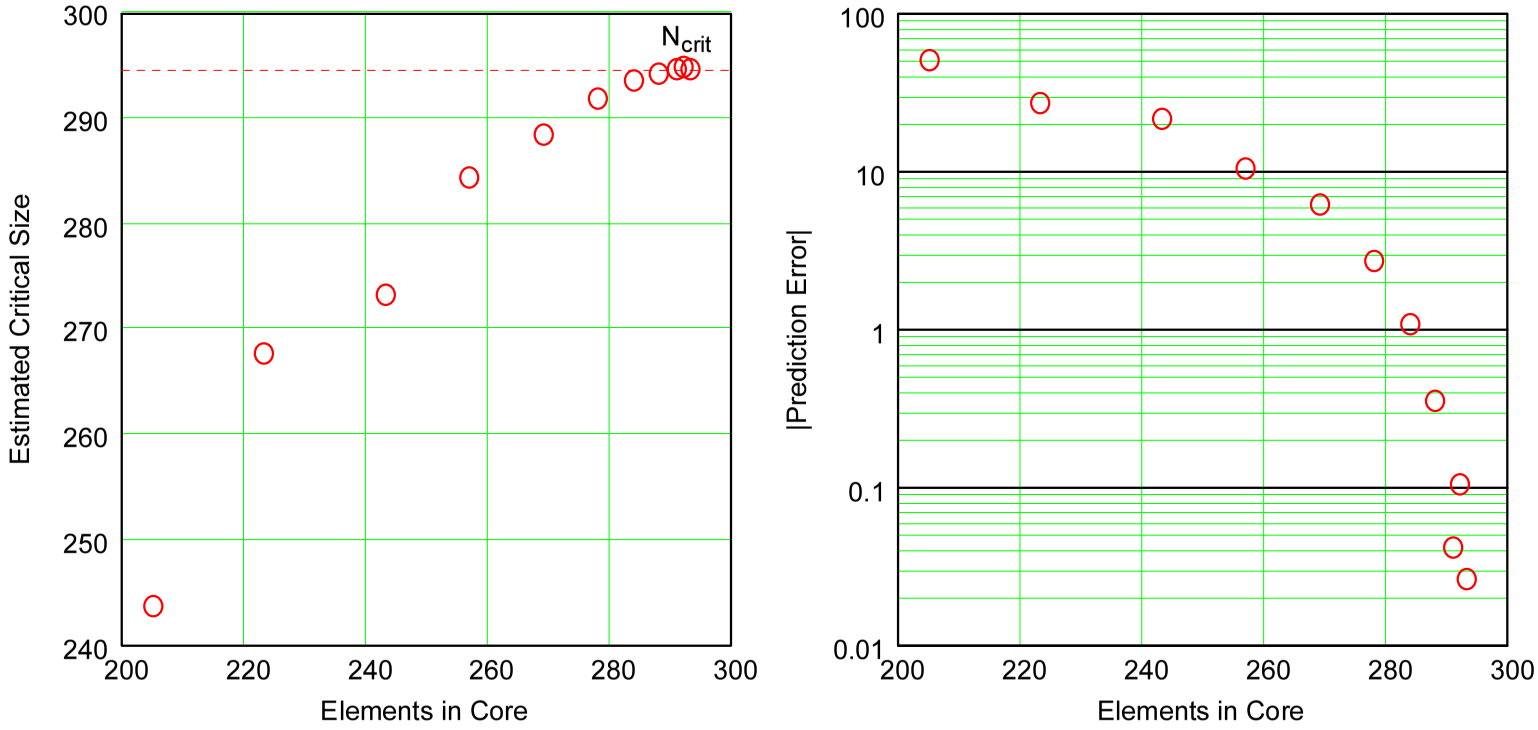

Figure 6-2. Estimated critical array size and the magnitude of the difference between the final critical array size and the successive estimates as a function of number of fuel elements in the assembly.

Where it was possible, the experiments were loaded with the same fuel element in each location. For example, core configuration 1 above was converted into configuration 2 by replacing the 36 driver fuel elements surrounding the central source element with 36 experiment fuel elements that contained no foils. All other grid locations contained the identical fuel elements from configuration 1. Similarly, configuration 5 differed from configuration 2 by the 36 experiment fuel elements containing rhodium foils and the addition of several driver fuel elements necessary to overcome the negative reactivity of the rhodium foils. The fuel element differences between configurations 2 and 5 are shown in Figure 6-3. The fuel element differences between configurations 7 and 10 are shown in Figure 6-4.

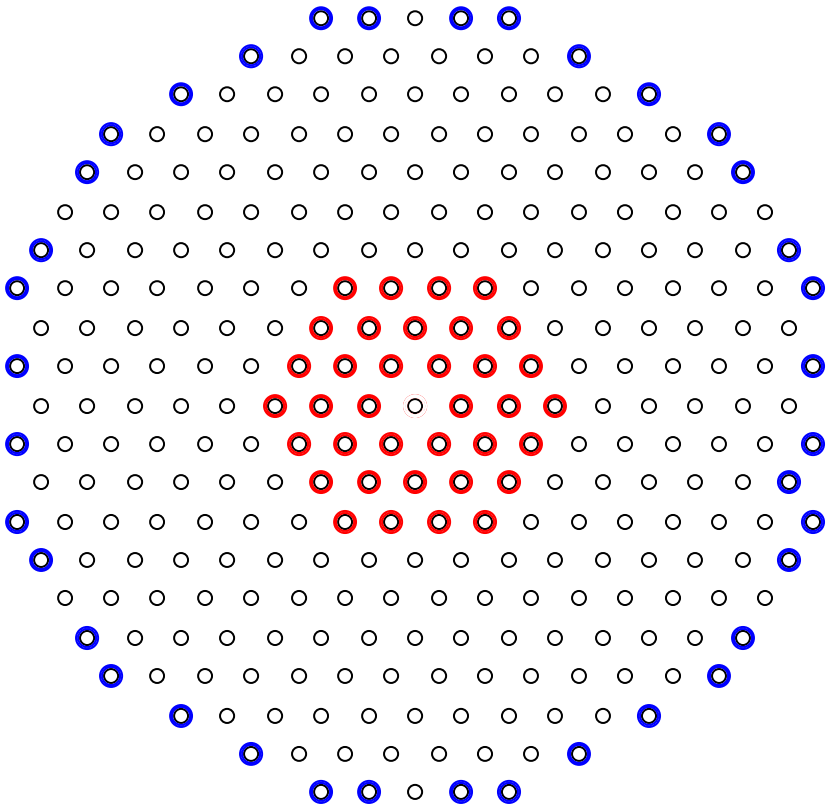

Figure 6-3. Fuel element configuration of the core with 2.0 cm pitch and 100 micron rhodium foils. Locations that had different loading from the configuration with no foils are highlighted. The 36 locations surrounding the central element contained different experiment fuel elements. The highlighted locations around the periphery indicate the driver fuel elements added to compensate for the negative reactivity of the rhodium foils.

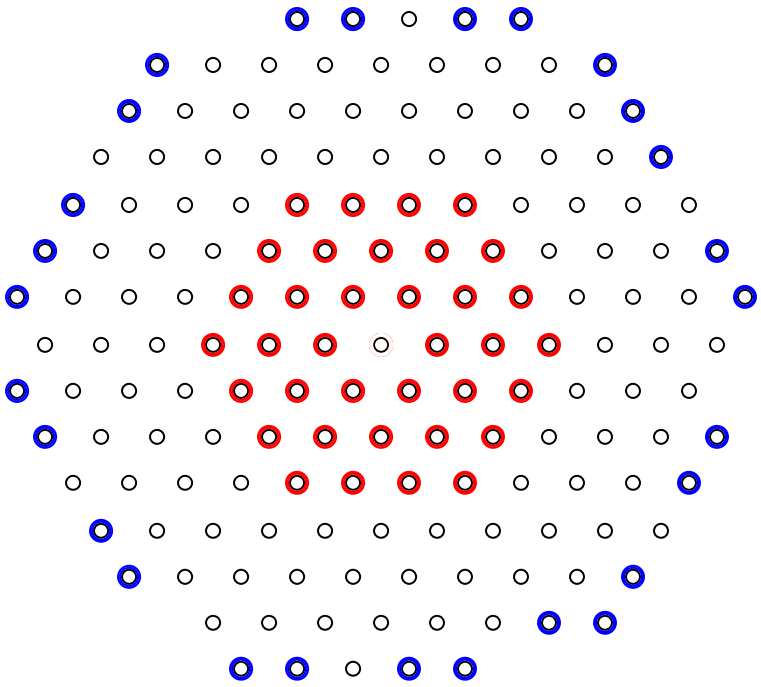

Figure 6-4. Fuel element configuration of the core with 2.8 cm pitch and 100 micron rhodium foils. Locations that had different loading from the configuration with no foils are highlighted. The 36 locations surrounding the central element contained different experiment fuel elements. The highlighted locations around the periphery indicate the driver fuel elements added to compensate for the negative reactivity of the rhodium foils.

The rhodium used in the experiment was 99.9% pure. Assuming a nominal density for the rhodium of 12.40 g/cm^3, the actual foil thicknesses based on the aggregate measured foil masses, were 25.2, 49.7 and 105.0 microns.

The experiments were run with the moderator temperature held at approximately 300 K. The last few steps of the two experiments that had 36 experiment fuel elements but no foils were repeated at a slightly elevated temperature to determine the magnitude of any temperature correction needed to obtain results at a constant temperature.

6.3. Experiment Results

The ten critical experiments were done using the method described above. The results of the ten critical experiments are shown in Table 6-1. The reported results are corrected to a temperature of 300 K. The uncertainties reported with the critical array sizes are based on the uncertainty due to the counting statistics in the count rate data added in quadrature to the uncertainty in the temperature correction to 300 K.

In some of the critical experiments, count-rate measurements were not done above a certain fuel loading because the settling time in the count rate was excessive. The largest array size for which count-rate data were taken is shown in Table 6-2. Also shown is the eigenvalue (k_{eff}) of the last measured configuration. The eigenvalues were obtained by multiplying the fuel element difference between the loading at critical and the last measured configuration by the incremental fuel element worth as calculated with MCNP4C (LANL 2000) and subtracting from unity. Given these eigenvalues, the multiplication of the last measured configuration was calculated and is also shown in the table. The maximum multiplication ranged from a low of 685 to a high of 2381.

These results can be compared to the results of an analysis method by doing a simulated approach-to-critical by analysis and comparing the measured critical array size with the calculated critical array size. However, this requires that calculations be made for a number of different array configurations and an interpolation done between the calculated data points.

Table 6-1. Critical array sizes measured during the ten critical experiments. The uncertainties shown account only for uncertainties in the critical array size measurement due to counting statistics and the temperature correction.

Number of Experiment Elements	Foil Thickness (mm)	2.0 cm pitch Measured Critical Size (elements)	2.8 cm Pitch Measured critical size (elements)
0	-	258.29 ± 0.03	132.30 ± 0.03
36	0	258.09 ± 0.02	131.97 ± 0.03
36	0.0252	270.67 ± 0.03	140.56 ± 0.03
36	0.0497	279.62 ± 0.03	146.88 ± 0.03
36	0.1050	294.75 ± 0.03	158.59 ± 0.03

Table 6-2. The largest array size measured for each experiment configuration. Also listed is the eigenvalue and multiplication for each configuration.

Number of Experiment Elements	Foil Thickness (mm)	2.0 cm Pitch			2.8 cm Pitch		
		Fuel Elements	k_{eff}	Multi-plication	Fuel Elements	k_{eff}	Multi-plication
0	-	257	0.99896	962	132	0.99953	2128
36	0	257	0.99915	1176	131	0.99854	685
36	0.0252	270	0.99951	2041	140	0.99922	1282
36	0.0497	279	0.99958	2381	146	0.99875	800
36	0.1050	294	0.99948	1923	158	0.99922	1282

A more straightforward comparison between experiment and calculation can be done if the eigenvalue of a specific experimental configuration with an integer number of fuel elements can be determined. This can be done by first calculating the incremental fuel element worth near the measured critical array size and multiplying that worth with the fractional difference in fuel elements between the measured critical configuration and the one to be calculated. For example, the critical configuration for the experiment with no experiment fuel elements and a pitch of 2.0 cm is most closely approximated by an array of 258 fuel elements. The incremental worth of a fuel elements at this array size is calculated to be 0.00074 ± 0.00003 for that array size. The 0.29 element deficit then translates to a reactivity deficit of 0.00021 giving an eigenvalue of 0.99979 for that configuration. Table 6-3 lists the eigenvalues for configurations approximating the measured critical arrays for the ten critical experiments. The uncertainties here are based on the sum in quadrature of the uncertainty due to the counting statistics in the count rate data, the uncertainty in the temperature correction to 300 K, and the uncertainty in the calculation of the worth of the incremental fuel element from the Monte Carlo statistics.

6.4. Experiment Uncertainties

As noted, the uncertainties reported above account only for the counting statistics and the uncertainty in the temperature correction. There are many other sources of uncertainty in critical experiments such as these. These sources of uncertainty can include tolerances on the dimensions of the parts of the assembly (e.g. pitch, fuel element OD, etc.), uncertainties in the amount of fissile material present (e.g. mass of fuel, enrichment, fuel stoichiometry, etc.), uncertainties in the composition of the assembly parts (e.g. clad, grid plates, etc.), and uncertainties in the measured temperature of the assembly.

To estimate the magnitude of the uncertainties in the experiment, a series of KENO-V.a (ORNL 2000) calculations was done that included various perturbations of the nominal configuration of the assembly to get the sensitivity of the assembly eigenvalue to the various uncertainty sources. The estimated uncertainties for the experiments are shown graphically in Figure 6-5. Because the sources of uncertainty are uncorrelated, the proper way to get a total uncertainty in the experiments is to add them in quadrature.

For the experiments with a pitch of 2.0 cm, the estimated uncertainty is 0.00147±0.00001. The accuracy of the uncertainty is based solely on the Monte Carlo statistics of the sensitivity

Table 6-3. Eigenvalues for configurations with integral fuel arrays. The uncertainties shown account only for uncertainties due to counting statistics, the temperature correction, and statistical uncertainty in the fuel element worth calculations.

Number of Experiment Elements	Foil Thickness (mm)	2.0 cm Pitch		2.8 cm Pitch	
		Fuel Elements	Eigenvalue	Fuel Elements	Eigenvalue
0	-	258	0.99979±0.00002	132	0.99954±0.00004
36	0	258	0.99993±0.00002	132	1.00004±0.00004
36	0.0252	271	1.00025±0.00002	141	1.00065±0.00004
36	0.0497	280	1.00026±0.00002	147	1.00018±0.00004
36	0.1050	295	1.00018±0.00002	159	1.00054±0.00004

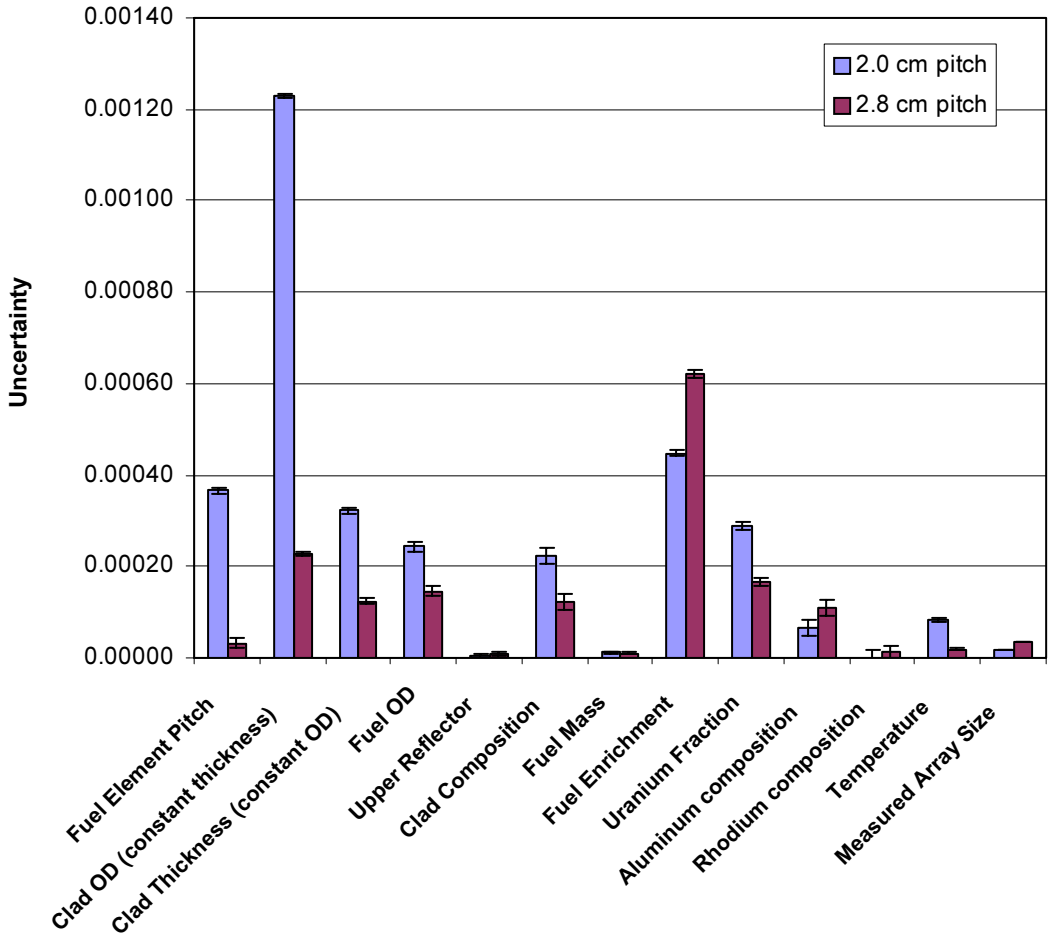

Figure 6-5. Sources of uncertainty in the experiments when the experiments are compared with unrelated critical experiments.

calculations. The uncertainty in this under-moderated assembly is due primarily to uncertainties in the fuel-to-water ratio from the uncertainties in the clad OD and the fuel element pitch.

For the experiments with a pitch of 2.8 cm, the estimated uncertainty is 0.00073±0.00001. The accuracy of the uncertainty is again based solely on the Monte Carlo statistics of the sensitivity calculations. For these nearly optimally moderated assemblies, the source of the largest uncertainty is from the fissile content of the fuel due to enrichment uncertainties.

In the analysis of the experiment uncertainties described above, all sources of uncertainty are fully considered. This is appropriate when the results of the experiments are compared to unrelated experiments (e.g. critical experiments not done as part of this project). However, when comparisons are made between the experiments described here, that method overestimates the actual uncertainties. Many aspects of the experiments are constant from one experiment to another. For example, the different cores have a given fuel element in the same position as described above. Only the fuel elements that change from core to core need

be considered in the uncertainty. When comparing configuration 5 with configuration 2, only the uncertainties arising from the fuel elements highlighted in Figure 6-3 need be included. The various uncertainties obtained in this way are shown in Figure 6-6. The aggregate uncertainties are 0.00030±0.00001 for the 2.0 cm pitch experiments and 0.00040±0.00001 for the 2.8 cm pitch experiments.

The measured critical array sizes for the ten experiment configurations and the uncertainties for both unrelated and correlated experiments are shown in Table 6-4. The eigenvalues and similar uncertainties for integral fuel arrays are shown in Table 6-5.

6.5. Experiment Biases

Normally, the models of critical experiments that are used to benchmark codes are simplified to decrease the level of effort required to model the experiment. There are several candidate

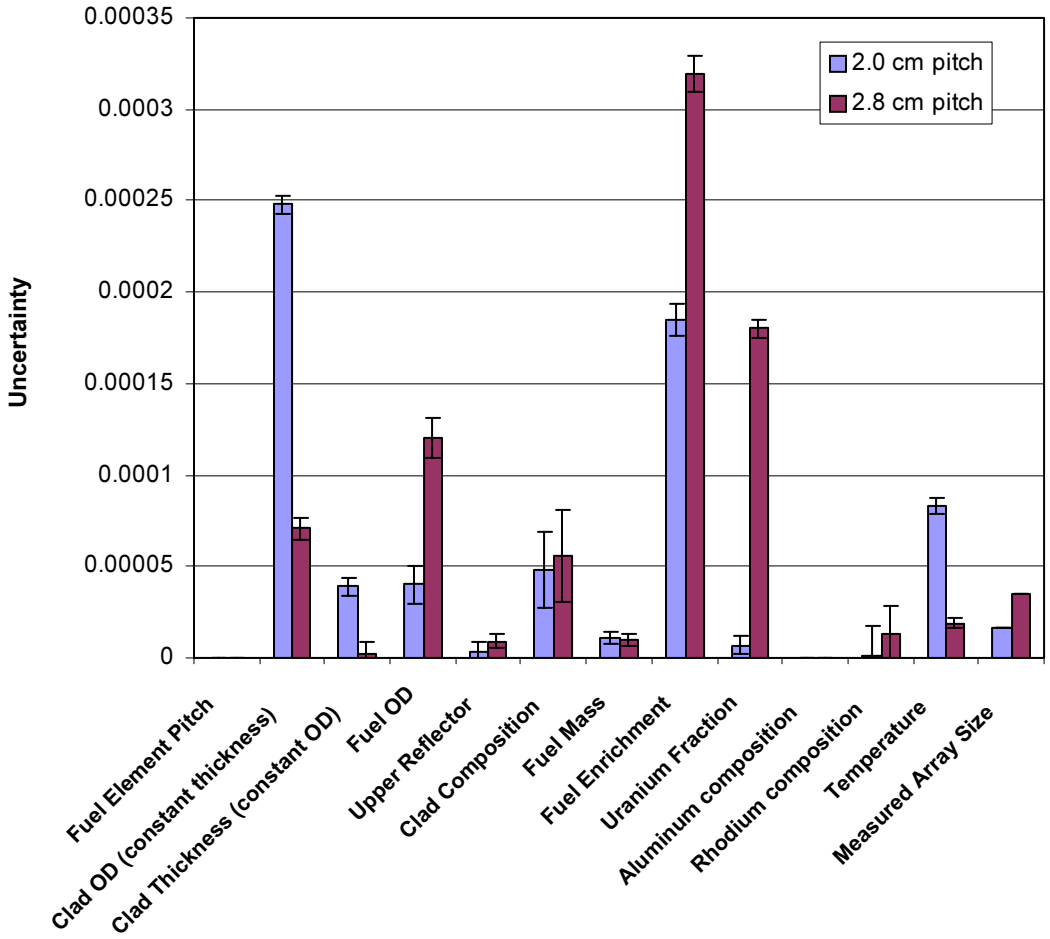

Figure 6-6. Sources of uncertainty in the experiments when experiments at a given pitch are compared with other experiments in the same set.

Table 6-4. Measured critical array sizes for the ten critical experiments with uncertainty estimates. The first column of uncertainties is for use when comparing these experiments with unrelated experiments. The second column of uncertainties is for use when making comparisons between the experiments reported here.

Pitch (cm)	Number of Expt. Elements	Foil Thickness (mm)	Measured Critical Array Size (elements)	Uncertainty for Unrelated Experiments (elements)	Uncertainty for Correlated Experiments (elements)
2.0	0	-	258.29	2.00	0.45
	36	0	258.09	1.89	0.42
	36	0.0252	270.67	1.96	0.44
	36	0.0497	279.62	2.13	0.48
	36	0.1050	294.75	2.01	0.45
2.8	0	-	132.30	0.48	0.26
	36	0	131.97	0.46	0.25
	36	0.0252	140.56	0.50	0.27
	36	0.0497	146.88	0.50	0.27
	36	0.1050	158.59	0.55	0.30

Table 6-5. Eigenvalues for integral model arrays of the ten critical experiment configurations with uncertainty estimates. The first column of uncertainties is for use when comparing these experiments with unrelated experiments. The second column of uncertainties is for use when making comparisons between the experiments reported here.

Pitch (mm)	Number of Expt. Elements	Foil Thickness (mm)	Model Size (elements)	Model k_{eff}	Uncertainty for Unrelated Experiments	Uncertainty for Correlated Experiments
2.0	0	-	258	0.99979	0.00147	0.00033
	36	0	258	0.99993	0.00147	0.00033
	36	0.0252	271	1.00025	0.00147	0.00033
	36	0.0497	280	1.00026	0.00147	0.00033
	36	0.1050	295	1.00018	0.00147	0.00033
2.8	0	-	132	0.99954	0.00073	0.00040
	36	0	132	1.00004	0.00073	0.00040
	36	0.0252	141	1.00065	0.00073	0.00040
	36	0.0497	147	1.00018	0.00073	0.00040
	36	0.1050	159	1.00054	0.00073	0.00040

simplifications to be considered for these experiments. Each simplification introduces a bias, hopefully small, into the model. The following simplifications were considered:

1. Elimination of the fuel element springs. Each fuel element has a corrosion-resistant spring at the top of the fuel column.
2. Replacing the central source fuel element with a driver fuel element. The neutron source that was used to drive the subcritical configurations of the experiment was in a stainless steel capsule that was at the midplane of the fuel in the central source rod.
3. Elimination of the polyethylene-filled projections of the experiment fuel elements.

4. Replacing the control/safety elements with driver fuel elements.
5. Filling the threaded holes in the ends of the fuel elements with cladding material.
6. Filling the lateral grooves in the fuel element end plugs with cladding materials.

The bias introduced by each listed simplification was calculated. The first two each introduced a positive bias while the remainder each introduced a small bias that was comparable to the uncertainty in the analysis. The bias introduced by each of the simplifications is shown in Figure 6-7. The sum of all the biases for the 2.0 cm pitch experiments is 0.00026±0.00007. The sum for the 2.8 cm pitch experiments is

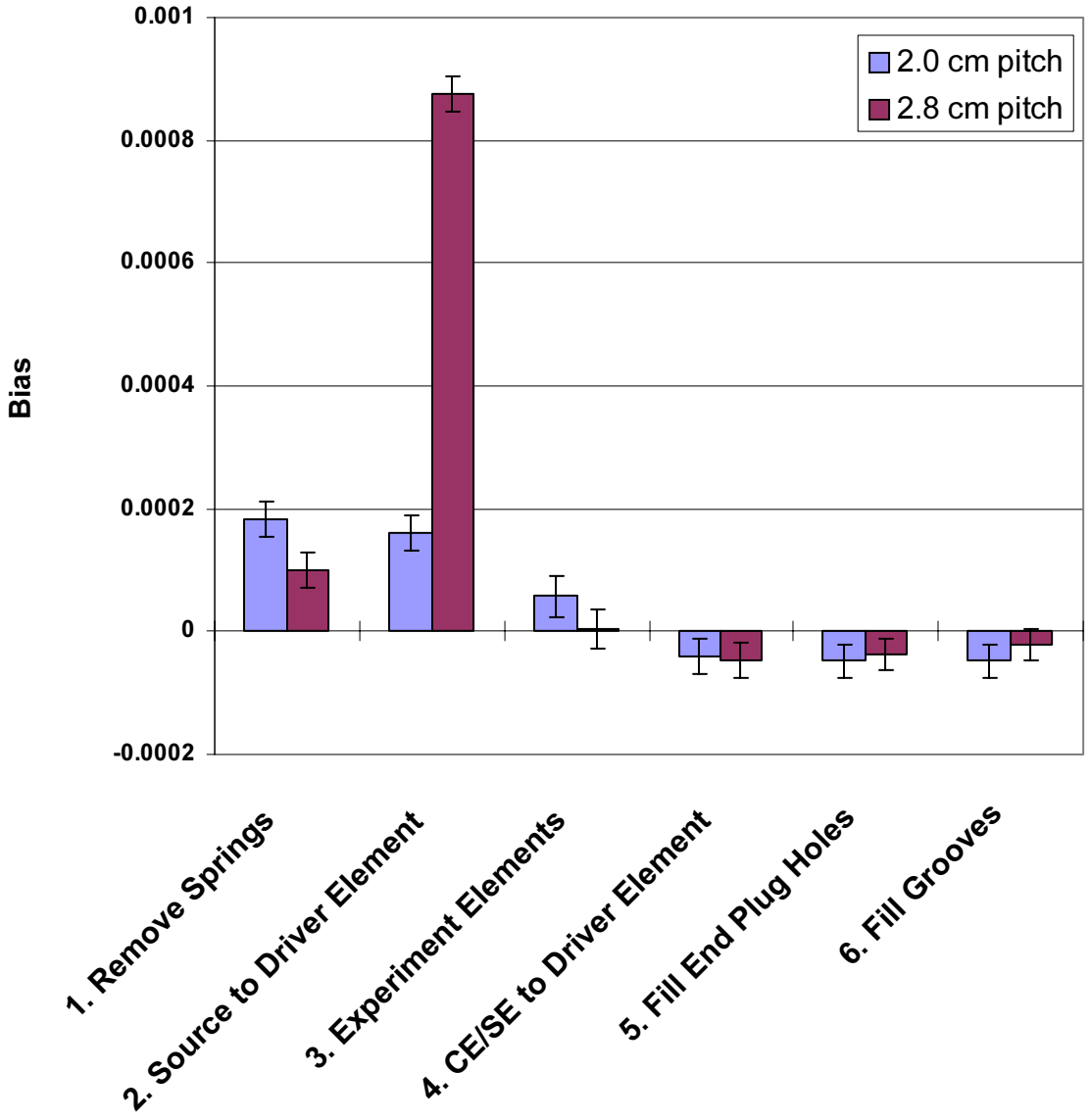

Figure 6-7. Biases that account for simplifications in the benchmark calculational model from the actual configuration.

0.00087±0.00007. The eigenvalues including bias for simplified models of the ten critical experiments are shown in Table 6-6.

Table 6-6. Eigenvalues including biases for simplified models of integral arrays of the ten critical experiment configurations with uncertainty estimates. The first column of uncertainties is for use when comparing these experiments with unrelated experiments. The second column of uncertainties is for use when making comparisons between the experiments reported here.

Pitch (mm)	Number of Expt. Elements	Foil Thickness (mm)	Model Size (elements)	Model k_{eff}	Uncertainty for Unrelated Experiments	Uncertainty for Correlated Experiments
2.0	0	-	258	1.00005	0.00147	0.00034
	36	0	258	1.00019	0.00147	0.00034
	36	0.0252	271	1.00051	0.00147	0.00034
	36	0.0497	280	1.00053	0.00147	0.00034
	36	0.1050	295	1.00044	0.00147	0.00034
2.8	0	-	132	1.00041	0.00073	0.00040
	36	0	132	1.00092	0.00073	0.00040
	36	0.0252	141	1.00152	0.00073	0.00040
	36	0.0497	147	1.00106	0.00073	0.00040
	36	0.1050	159	1.00142	0.00073	0.00040

7. Comparison With Analysis

The scope of the project as proposed included the measurement of the benchmark data but did not include the comparison of the measurements with calculations. However, a considerable suite of calculations was done in the safety analysis and uncertainty analysis for the experiment. The following sections that compare the experiment results to the results of two analytical methods are included for two reasons:

1. The comparisons demonstrate the use of the experimental data to test analytical methods.
2. The comparisons, in part, demonstrate the quality of the data taken as part of the project.

In that spirit, the following sections are offered.

7.1. The Experiments as Criticality Safety Benchmarks

7.1.1. Comparison With MCNP4C

The Monte Carlo transport code MCNP4C (LANL 2000), its predecessors and its progeny are standard tools used in criticality safety work. MCNP4C was used extensively to design and analyze the critical experiments reported here. The benchmark configurations reported above were analyzed and the calculated eigenvalues (k_{eff}) are given in Table 7-1. The model of the critical assembly was sufficiently detailed to warrant comparison with the experimental results presented in Table 6-5. The difference (Δk_{eff}) between the calculated and measured k_{eff} is also shown in the table for each configuration. The Δk_{eff}s with uncertainties are shown graphically in Figure 7-1. The average Δk_{eff} for the experiments at each pitch with the standard deviation is also shown in the table.

As can be seen in Table 7-1 and Figure 7-1, the Δk_{eff}s for the experiments cluster around different average values that depend on the fuel element pitch. When the uncertainties for uncorrelated experiments are included, the results overlap.

A series of 70 criticality benchmarks from (NEA 2002) using UO_2 fuel with enrichment less than 5% was analyzed using the same code and cross sections. Using the terminology of the reference, the benchmarks came from experiments LEU-COMP-THERM-001, -002, -008, -009, -010, -014, -016, -042, and -052. The average difference between the calculated k_{eff} and that reported for the 73 configurations was -0.0064 with a standard deviation of 0.0012. The Δk_{eff}s for the experiments reported here are consistent with that result when experimental uncertainties are considered.

7.1.2. Comparison with SCALE 4.4a

The Monte Carlo transport code KENO V.a (ORNL 2000) has been a standard tool used in criticality safety work for many years. KENO V.a was also used to analyze the critical experiments reported here. The benchmark configurations reported above were analyzed and the calculated eigenvalues (k_{eff}) are given in Table 7-2. The model of the critical assembly was sufficiently detailed to warrant comparison with the experimental results presented in

Table 7-1. Results of MCNP4C calculations for the ten critical experiments.							
Pitch (mm)	**Experiment Elements**	**Foil Thickness (mm)**	**Model Elements**	**Calculated k_{eff} (note 1)**	**Uncer-tainty (note 2)**	**Δk_{eff} (C-E) (note 3)**	**Uncer-tainty (note 4)**
2.0	0	-	258	0.99191	0.00007	-0.00786	0.00147
	36	0	258	0.99199	0.00007	-0.00794	0.00147
	36	0.0252	271	0.99218	0.00007	-0.00807	0.00147
	36	0.0497	280	0.99242	0.00007	-0.00784	0.00147
	36	0.1050	295	0.99218	0.00007	-0.00799	0.00147
				Average		-0.00794	**(note 5)**
				Standard Deviation		0.00009	
2.8	0	-	132	0.99308	0.00007	-0.00645	0.00073
	36	0	132	0.99442	0.00007	-0.00562	0.00073
	36	0.0252	141	0.99458	0.00007	-0.00603	0.00074
	36	0.0497	147	0.99393	0.00007	-0.00625	0.00073
	36	0.1050	159	0.99444	0.00007	-0.00610	0.00074
				Average		-0.00609	**(note 5)**
				Standard Deviation		0.00031	
Both				**Average**		-0.00701	**(note 5)**
				Standard Deviation		0.00100	

Note 1: k_{eff} is the eigenvalue reported by MCNP4C using cross sections from ENDF/B-VI data.

Note 2: This uncertainty accounts only for the stochastic nature of the calculations.

Note 3: Δk_{eff} is the difference between the calculated array k_{eff} and the experimental array k_{eff} reported in Table 6-5.

Note 4: This uncertainty is the sum in quadrature of the statistical uncertainty in the calculations and the uncertainty in the measured k_{eff} for uncorrelated experiments.

Note 5: The averages and standard deviations are based solely on the Δk_{eff}s and do not account for the experimental uncertainties.

Table 6-5. The difference (Δk_{eff}) between the calculated and measured k_{eff} is also shown in the table for each configuration. The Δk_{eff}s with uncertainties are shown graphically in Figure 7-2. The average Δk_{eff} for the experiments at each pitch with the standard deviation is also shown in the table.

As can be seen in Table 7-2 and Figure 7-2, the Δk_{eff}s for the experiments cluster around different average values that depend on the fuel element pitch. In contrast with the MCNP4C results, when the uncertainties for uncorrelated experiments are included, the average values are significantly different. As noted above, determination of the cause of the discrepancy is beyond the scope of this project.

A series of 70 criticality benchmarks from (NEA 2002) using UO_2 fuel with enrichment less than 5% was analyzed using the same code and cross sections. Using the terminology of the reference, the benchmarks came from experiments LEU-COMP-THERM-001, -002, -008, -009, -010, -014, -016, -042, and -052. The average difference between the calculated k_{eff} and

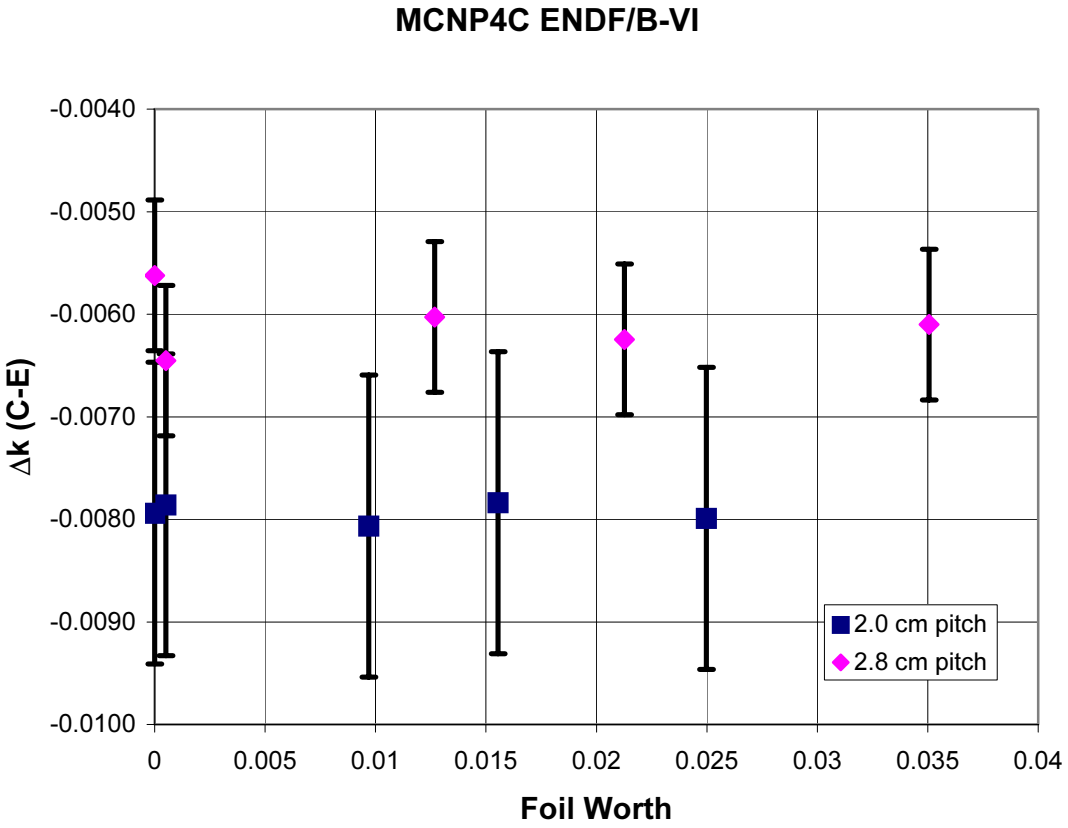

Figure 7-1. Bias in the MCNP4C calculations for the ten critical experiments. The data for the experiment with no experiment elements is offset slightly from the axis for clarity.

that reported for the 73 configurations was -0.0059 with a standard deviation of 0.0030. The Δk_{eff}s for the experiments reported here are consistent with that result when experimental uncertainties are considered.

7.2. The Experiments as Tests of Rhodium Cross Sections

These experiments were designed so that the effect of a specific material could be isolated to allow the treatment of that material by an analytical method to be tested. At each fuel element pitch, two experiments were done to 1) provide baseline criticality data to "zero out" effects caused by materials other than the test material and 2) provide data on the effect on the array of the difference between the driver fuel elements and the experiment fuel elements. Experiments were also done with rhodium foils of different thicknesses inserted between the fuel pellets in the experiment fuel elements.

The effect of the rhodium foils on the assembly depended on the thickness of the foils. For each thickness, the "foil worth," defined as the calculated reactivity change that occurs when the experiment foils are voided, was calculated using both MCNP4C and KENO V.a. The

Table 7-2. Results of KENO V.a calculations for the ten critical experiments.							
Pitch (mm)	**Experiment Elements**	**Foil Thickness (mm)**	**Model Elements**	**Calculated k_{eff} (note 1)**	**Uncer-tainty (note 2)**	**Δk_{eff} (C-E) (note 3)**	**Uncer-tainty (note 4)**
2.0	0	-	258	0.99020	0.00004	-0.00957	0.00147
	36	0	258	0.99076	0.00005	-0.00917	0.00147
	36	0.0252	271	0.99081	0.00005	-0.00944	0.00147
	36	0.0497	280	0.99096	0.00004	-0.00930	0.00147
	36	0.1050	295	0.99094	0.00005	-0.00923	0.00147
					Average	-0.00934	**(note 5)**
					Standard Deviation	0.00016	
2.8	0	-	132	0.99391	0.00006	-0.00563	0.00073
	36	0	132	0.99474	0.00005	-0.00530	0.00073
	36	0.0252	141	0.99535	0.00005	-0.00526	0.00073
	36	0.0497	147	0.99474	0.00005	-0.00544	0.00073
	36	0.1050	159	0.99528	0.00005	-0.00526	0.00073
					Average	-0.00538	**(note 5)**
					Standard Deviation	0.00016	
Both					**Average**	-0.00736	**(note 5)**
					Standard Deviation	0.00210	

Note 1: k_{eff} is the eigenvalue reported by MCNP4C using cross sections from ENDF/B-VI data.
Note 2: This uncertainty accounts only for the stochastic nature of the calculations.
Note 3: Δk_{eff} is the difference between the calculated array k_{eff} and the experimental array k_{eff} reported in Table 6-5.
Note 4: This uncertainty is the sum in quadrature of the statistical uncertainty in the calculations and the uncertainty in the measured k_{eff} for uncorrelated experiments.
Note 5: The averages and standard deviations are based solely on the Δk_{eff}s and do not account for the experimental uncertainties.

foil worth for each configuration is listed in Table 7-3 for both sets of calculations. The MCNP4C results are shown in Figure 7-3 as a function of foil thickness. Several effects are visible in the figure. First, a given set of foils has a larger reactivity impact on the 2.8 cm pitch experiments than on the 2.0 cm pitch experiments. This is because the experiments at 2.8 cm pitch have a softer neutron spectrum because they are more optimally moderated and the fixed number of experiment rods is a larger fraction of the smaller cores. Second, the foil removal reactivity is sublinear as a function of foil thickness. This is due to self-shielding in the foils. Third, the reactivity worth of the rhodium foils is relatively large, up to 2.5% at 2.0 cm pitch and 3.5% at 2.8 cm pitch, giving a large signal relative to the experimental uncertainties.

The Δk_{eff}s given in Tables 7-1 and 7-2 give the overall bias of the analytical methods relative to the critical experiments. The average bias from the tables for MCNP4C is 0.75% and 0.74% for KENO V.a. The bias is due to the integration of inaccuracies in the modeling of the experiment, inaccuracies of the analytical method, and inaccuracies in the cross section

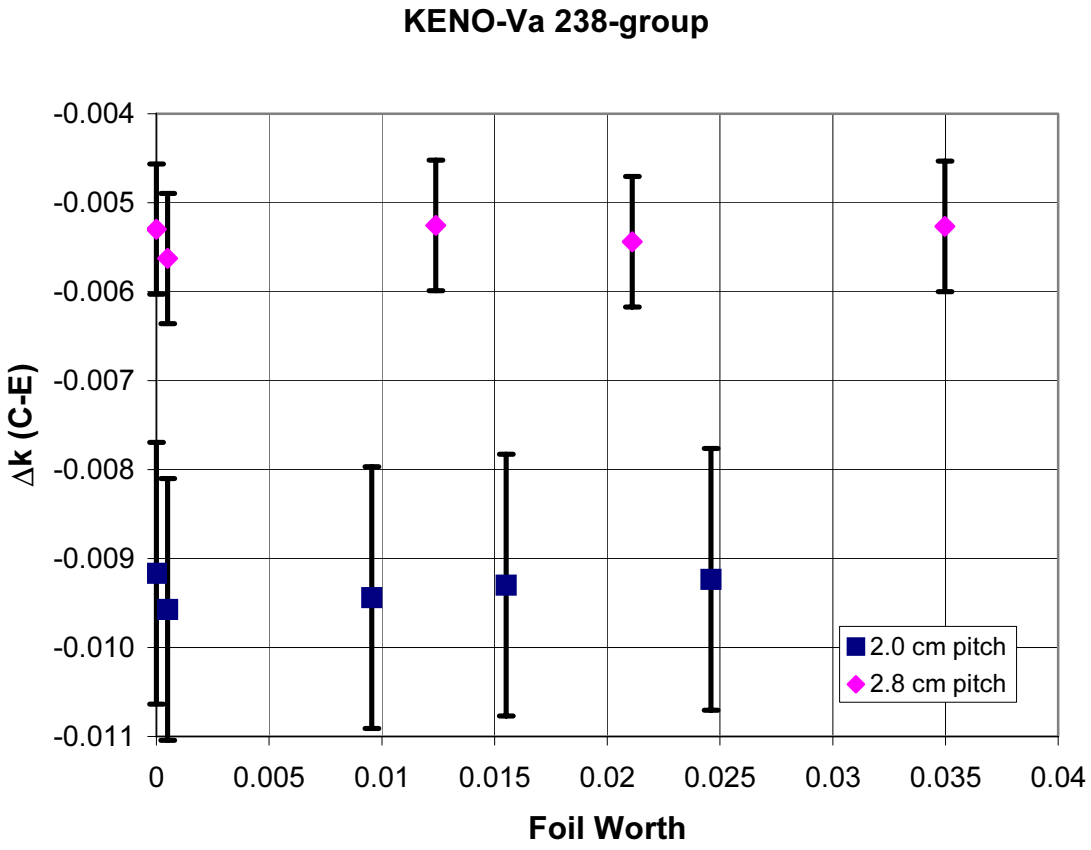

Figure 7-2. Bias in the KENO V.a calculations for the ten critical experiments. The data for the experiment with no experiment elements is offset slightly from the axis for clarity.

data. To test the accuracy of the treatment of one aspect of a calculational scheme, such as the accuracy of the treatment of rhodium, the biases from other sources must be removed. In the experiments reported here, that is done by comparing the reactivity difference between calculation and experiment for cases that contain the test material with cases that do not. Table 7-4 lists this reactivity difference ($\Delta\rho$) as calculated by MCNP4C and KENO V.a. Because the comparisons are made with experiments in this set, the appropriate experimental uncertainties to use are the smaller ones for correlated experiments. The ratio of the uncertainty in $\Delta\rho$ to the foil worth is the relative uncertainty in the rhodium reactivity and ranges from 1.2 to 3.3 percent. The relative uncertainties are small enough that the experiments can serve as good tests of the analysis of rhodium in the critical experiments.

The $\Delta\rho$s for MCNP4C are shown in Figure 7-4. The $\Delta\rho$s for KENO V.a are shown in Figure 7-5. When the overall bias is removed, the $\Delta\rho$s for all the experiments are within the experimental uncertainty of zero. There is no discernable trend as a function of foil thickness. Both MCNP4C and KENO V.a reproduce the effect of the rhodium on the experiment within the experimental uncertainties.

Table 7-3. Rhodium foil worth calculated by MCNP4C and KENO V.a for each of the critical experiments.

Pitch (mm)	Experiment Elements	Foil Thickness (mm)	Model Elements	MCNP4C		KENO V.a	
				Foil Worth (note 1)	Uncer-tainty (note 2)	Foil Worth (note 1)	Uncer-tainty (note 2)
2.0	0	-	258	0	0	0	0
	36	0	258	0	0	0	0
	36	0.0252	271	0.00969	0.00012	0.00908	0.00008
	36	0.0497	280	0.01554	0.00012	0.01497	0.00008
	36	0.1050	295	0.02497	0.00012	0.02378	0.00007
2.8	0	-	132	0	0	0	0
	36	0	132	0	0	0	0
	36	0.0252	141	0.01268	0.00012	0.01210	0.00007
	36	0.0497	147	0.02127	0.00012	0.02070	0.00007
	36	0.1050	159	0.03506	0.00012	0.03458	0.00006

Note 1: This is the calculated reactivity difference between the array with the foils voided and the actual array.

Note 2: This uncertainty is the summed uncertainties in the calculations used to obtain the Foil Removal Reactivity.

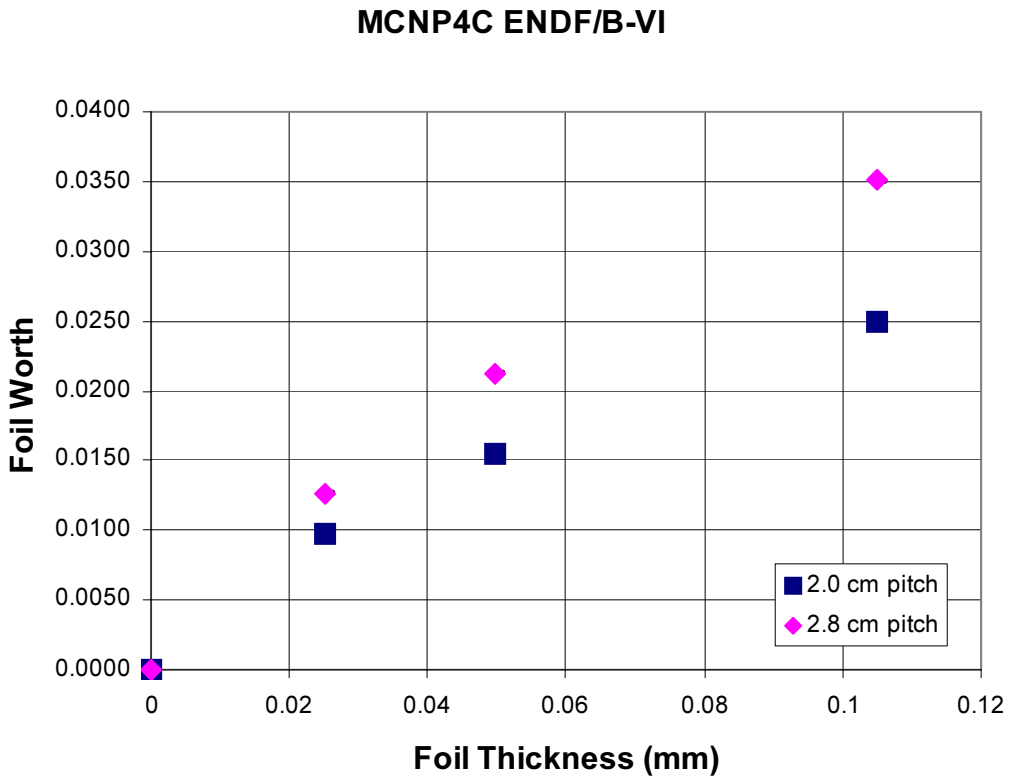

Figure 7-3. Rhodium foil worth as a function of foil thickness calculated by MCNP4C.

Table 7-4. Reactivity difference between calculated and measured results for the ten critical experiments.

Pitch (mm)	Experiment Elements	Foil Thickness (mm)	Model Elements	MCNP4C			KENO V.a		
				Δρ (C-E) (note 1)	Uncer-tainty (note 2)	Relative Uncer-tainty (%) (note 3)	Δρ (C-E) (note 1)	Uncer-tainty (note 2)	Relative Uncer-tainty (%) (note 3)
2.0	0	-	258	0.00004	0.00031	0	-0.00021	0.00030	0
	36	0	258	-0.00004	0.00031	0	0.00021	0.00031	0
	36	0.0252	271	-0.00016	0.00031	3.2	-0.00006	0.00031	3.2
	36	0.0497	280	0.00007	0.00031	2.0	0.00008	0.00030	2.0
	36	0.1050	295	-0.00009	0.00031	1.2	0.00014	0.00031	1.2
2.8	0	-	132	-0.00042	0.00041	0	-0.00017	0.00041	0
	36	0	132	0.00042	0.00041	0	0.00017	0.00041	0
	36	0.0252	141	0.00002	0.00041	3.3	0.00022	0.00041	3.3
	36	0.0497	147	-0.00021	0.00041	1.9	0.00003	0.00041	1.9
	36	0.1050	159	-0.00005	0.00041	1.2	0.00021	0.00041	1.2

Note 1: Δρ is the reactivity difference between the calculated array k_{eff} and the experimental array k_{eff} with the average reactivity difference for the two arrays with no foils subtracted.

Note 2: This uncertainty is the sum in quadrature of the statistical uncertainty in the calculated array reactivity and the uncertainty in the measured array reactivity for correlated experiments.

Note 3: The relative uncertainty is the ratio of the uncertainty in Δρ and the foil worth from Table 7-3.

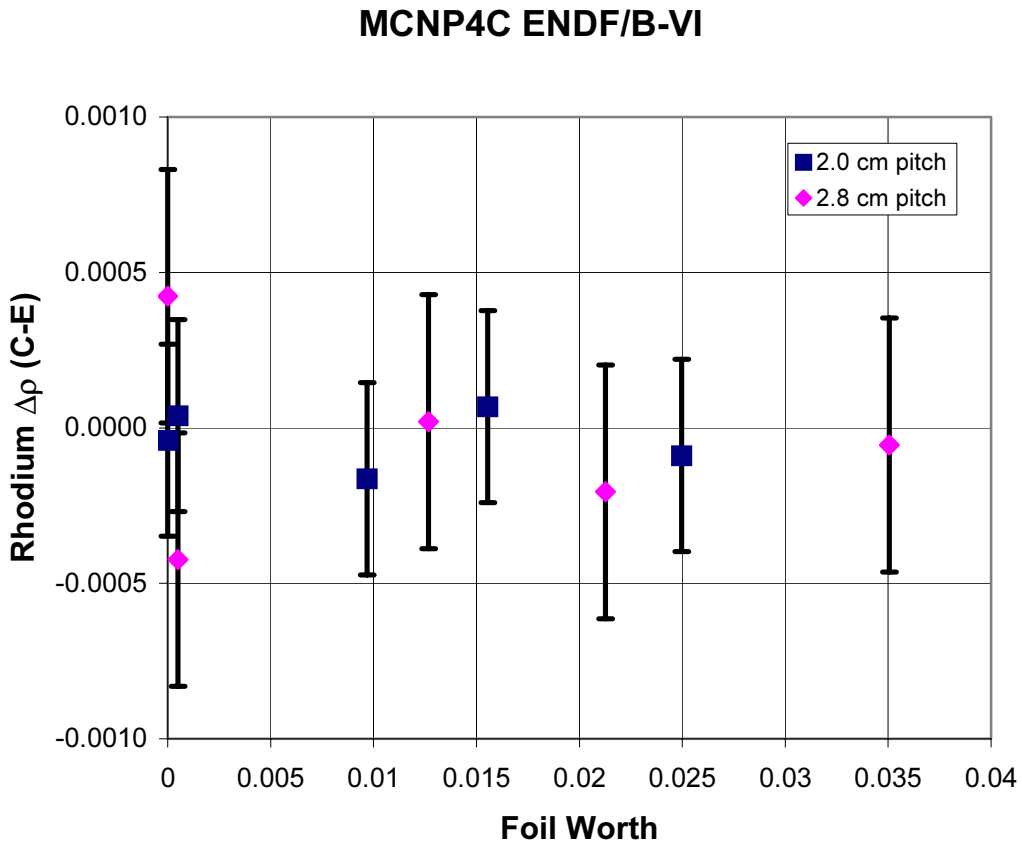

Figure 7-4. Reactivity difference between the MCNP4C calculations and the measurements for the ten critical experiments. The data for the experiment with no experiment elements is offset slightly from the axis for clarity.

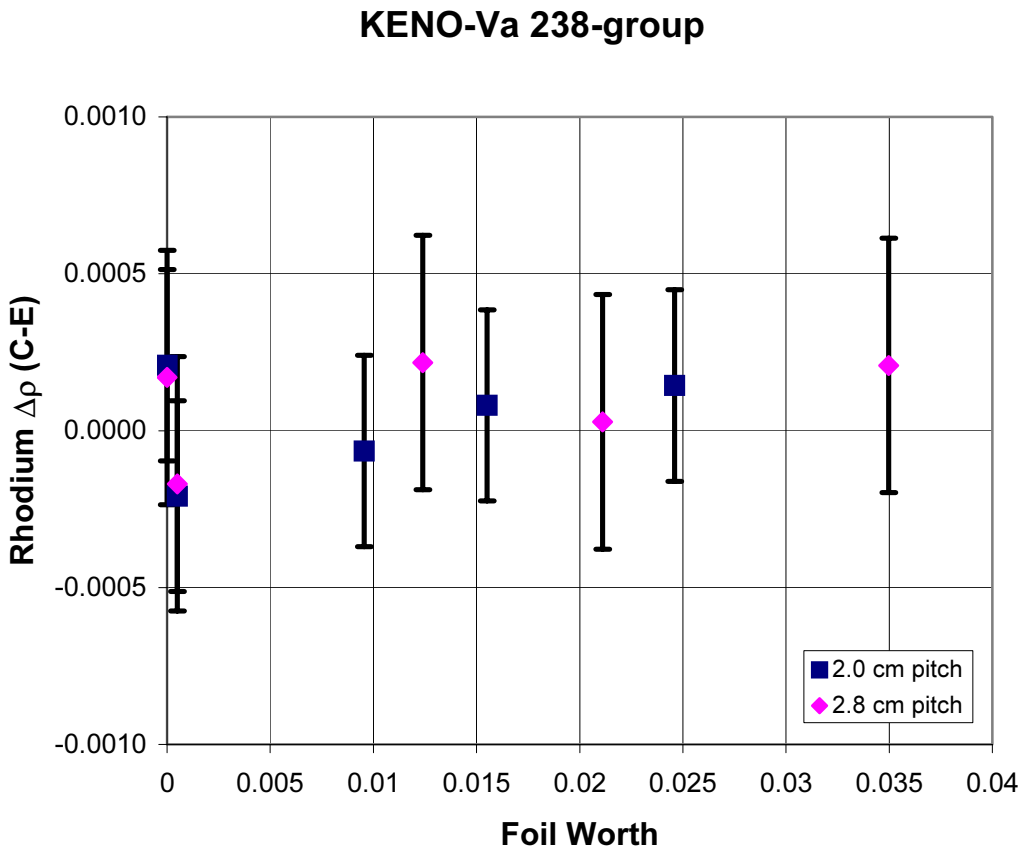

Figure 7-5. Reactivity difference between the KENO V.a calculations and the measurements for the ten critical experiments. The data for the experiment with no experiment elements is offset slightly from the axis for clarity.

8. Conclusion

This report has described NERI project 99-0200, *Experimental Investigation of Burn-up Credit for Safe Transport, Storage, and Disposal of Spent Nuclear Fuel* under which the Burnup Credit Critical Experiment (BUCCX) was conducted. The intent of the project was to accomplish two goals: to establish a critical experiment capability at Sandia that can address benchmark experiments relevant to the issues of commercial nuclear power and to demonstrate that capability by performing measurements with rhodium, an important fission product absorber, in the critical experiment. The project achieved both goals.

To accommodate the critical experiments, an authorization basis envelope for water-moderated low-enriched critical experiments was developed at the Sandia Pulsed Reactor Facility. An addendum to the facility safety analysis report was written to address the safety issues associated with critical experiments. Technical Safety Requirements were developed. Experiment operating procedures were written. These documents were subjected to a rigorous review process and approved by the appropriate authorities. The revised authorization basis envelope approved as part of the project will benefit future experiments of this type.

A critical assembly that can accommodate the project experiments was developed. While the design concept of the assembly hardware was based on an earlier experiment, much of the hardware from the earlier assembly was replaced. An enabling factor for this project was the fact that a large number of fuel elements useful for the experiments had been fabricated as part of an earlier project. The remaining special fuel elements necessary for the critical assembly were fabricated as part of the project. Another enabling factor was the existence of an instrumentation and control system used by an earlier critical experiment. The critical experiment hardware is another part of the legacy of the project.

Ten critical experiments were conducted as part of this project. Five were performed with a fuel to water ratio that was significantly undermoderated and comparable to that of commercial reactor fuel assemblies. Another five were performed with a fuel to water ratio that produced nearly optimal moderation. Each of the experiments can stand alone as a criticality benchmark. As such, the experimental uncertainties in the k_{eff} of the benchmark configurations were 0.0015 for the undermoderated experiments and 0.0009 for the optimally moderated experiments. These uncertainties compare very well with the uncertainties for other critical experiments in the literature.

With appropriate treatment, the effect of the rhodium on the critical experiments can be isolated as a function of the quantity of rhodium present for each set of five experiments. When the experiments are used this way, the experimental uncertainties decrease to 0.0003 for the undermoderated experiments and 0.0004 for the optimally moderated experiments. These uncertainties, combined with the calculated rhodium worth in the experiments give relative uncertainties in the rhodium worth of 1 to 3%.

The function of criticality safety benchmarks is to serve as tests of the analytical methods used in criticality safety calculations. The results of the critical experiments were compared to the results of two transport codes. The bias in the calculations when these experiments were modeled was similar to the bias in the codes when other critical experiments are

considered. Both codes predicted the rhodium behavior within the experimental uncertainties.

In addition to producing benchmark critical measurements and data on rhodium in critical systems, this project leaves intact a capability to perform low-enriched critical experiments at Sandia. A large fraction of the project resources was expended establishing this capability. Subsequent critical experiments can use the capability with a much-reduced up-front cost. There are a number of ways that this capability can be exploited. In fact, another NERI project using this capability, *Reactor Physics and Criticality Benchmark Evaluations for Advanced Nuclear Fuel* (01-124) was in progress when this report was written. Other possible uses of the critical experiment capability could be:

1. Measure the behavior of other fission products on a critical system. Such follow-on experiments could be used to provide the justification for the inclusion of fission product in the criticality analysis of spent fuel shipping, storage, and disposal configurations.
2. Measure static reactor physics parameters of critical systems with higher (e.g. >5%) enrichment such as are being done in NERI project 01-124. Such experiments could include measurements of fission density profiles, soluble poison reactivity worths, burnable poison rod reactivity worth, and others.
3. Examine the static reactivity behavior of new burnable poison types or configurations.
4. Perform critical experiments with variable enrichments to simulate the graded enrichments in BWR cores.
5. Examine cores with axially graded enrichment and possibly graded fission product content to simulate the end effects in spent nuclear fuel.
6. Perform critical experiments with Generation IV fuels and with transmutation fuels.
7. Examine the reactor physics behavior of transmutation targets.

These are examples of experiments that could be performed with the critical experiment capability established as part of this project. Many other studies are possible.

9. References

(DOE 1998) *Topical Report on Actinide-Only Burnup Credit for PWR Spent Nuclear Fuel Packages*, DOE/RW-0472, Rev. 2, U.S. Department of Energy, Office of Civilian Radioactive Waste Management, September 1998.

(LANL 2000) J. F. Briesmeister, ed., *MCNP™—A General Monte Carlo N-Particle Transport Code Version 4C*, LA-13709-M, Los Alamos National Laboratory, Los Alamos, New Mexico, April 10, 2000.

(Harms 1995) G. A. Harms, F. J. Davis, and J. T. Ford, *"The Spent Fuel Safety Experiment,"* Fifth International Conference on Nuclear Criticality Safety, ICNC '95, Albuquerque, NM, 1995.

(NEA 2002) NEA Nuclear Science Committee, *International Handbook of Evaluated Criticality Safety Benchmark Experiments*, NEA/NSC/DOC(95)03, Organization for Economic Cooperation and Development, Nuclear Energy Agency, September 2003.

(NRC 1999) Spent Fuel Project Office Interim Staff Guidance – 8, Rev. 1 – Limited Burnup Credit, U.S. Nuclear Regulatory Commission, July 30, 1999.

(ORNL 2000) *SCALE: A Modular Code System for Performing Standardized Computer Analyses for Licensing Evaluation*, NUREG/CR-0200, Rev. 6, Oak Ridge National Laboratory, Oak Ridge, TN, 2000.

(SNL 1989) Sandia National Laboratories, *Critical Assembly Safety Analysis Report*, SAND89-0851, Sandia National Laboratories, Albuquerque, NM, July 1989.

(SNL 2002a) Harms, Gary A., et. al, *Sandia Pulsed Reactor Facility Critical Experiments Addendum to the Sandia Pulsed Reactor Facility Safety Analysis Report*, SAND2002-1599, Sandia National Laboratories, Albuquerque, NM, 2002.

(SNL 2002b) Ford, John T., *Technical Safety Requirements for the Sandia Pulse Reactor Facility Critical Experiments*, SAND2002-1470, Sandia National Laboratories, Albuquerque, NM, 2002.

Distribution:

7 U. S. Department of Energy
Attn: Dr. Madeline Anne Feltus (5)
Lynn Hall (2)
Office of Nuclear Energy, Science & Technology
NE-20/Germantown Building
1000 Independence Ave., S.W.
Washington, D.C. 20585-1290

1 U. S. Department of Energy
Attn: Kenny K. Osborne
Idaho Operations Office
850 Energy Drive
Idaho Falls, ID 83401

3 U. S. Department of Energy
Attn: Dr. Thomas E. Kiess (2)
Dr. Robert Budnitz (1)
RW-40E/Forestal Bldg.
1000 Independence Ave., SW
Washington, D.C. 20585

1 U. S. Department of Energy
Attn: Nancy Slater-Thompson
RW-30E/Forestal Bldg.
1000 Independence Ave., SW
Washington, D.C. 20585

2 U. S. Department of Energy
Attn: William Mullen (1)
Kevin Gray (1)
National Nuclear Security Administration
Sandia Site Office
P. O. Box 5400
Kirtland Air Force Base
Albuquerque, NM 87185-1137

3 Oak Ridge National Laboratory
Attn: Bryan L. Broadhead (1)
Cecil V. Parks (1)
Bradley T. Rearden (1)
P. O. Box 2008, MS 6170
Oak Ridge, TN 37831-6170

1 Idaho National Engineering & Environmental Laboratory
Attn: J. Blair Briggs
2525 Fremont Avenue
P. O. Box 1625, MS 3860
Idaho Falls, ID 83415

2 Pacific Northwest National Laboratory
Attn: M. C. Brady Raap (1)
Robert J. Talbert (1)
P. O. Box 999 / K8-34
Richland, WA 99352

2 Framatome Advanced Nuclear Power, Inc.
Attn: William Anderson (1)
Patrick M. O'Leary (1)
3315 Old Forest Road
Lynchburg, VA 24501

1 Framatome Advanced Nuclear Power, Inc.
Attn: Thomas W. Doering
4020 Riseley Lane
Charlotte, NC 28270

1 University of Florida
Attn: James S. Tulenko
202 NSC
P. O. Box 118300
Gainesville, FL 32611-8300

3 Argonne National Laboratory
Attn: Phillip J. Finck (1)
Edward K. Fujita (1)
Hussein S. Khalil (1)
9700 S. Cass Avenue
Argonne, IL 60439

1 BNFL, Inc.
Attn: Mr. Nigel T. Gulliford
Rutherford House – R101
Risley Warrington
Cheshire WA3 6AS
England

1 West Texas A&M University
Attn: Freddie J. Davis, PhD
Engineering Program Coordinator
Dept. of Mathematics, Physical Sciences, and Engineering
Box 60787
Canyon, TX 79016-0001

1 NuclearConsultants.Com
Attn: Dr. Dale B. Lancaster
320 South Corl Street
State College, PA 16801

1 Bechtel SAIC, LLC
Attn: Michael Anderson
9412 Hershey Lane
Las Vegas, NV 89134

2 Los Alamos National Laboratory
Attn: Charlene Cappiello (1)
Richard Anderson (1)
P. O. Box 1663
Los Alamos, NM 87545

1 U. S. Nuclear Regulatory Commission
Attn: Carl J. Withee
One White Flint North
11555 Rockville Pike
Rockville, MD 20852-2738

1 Duke Energy
Attn: James R. Thornton
3603 Furman Circle
Gastonia, NC 28056-1631

1 RENMAR Enterprises, Inc.
Attn: Samit K. Bhattacharyya
1429 Clyde Drive
Naperville, IL 60565

1 Brookhaven National Laboratory
Attn: Michael Todosow
Energy Sciences and Technology Department
MS 475B
Upton, NY 11973-5000

1 Studsvik Scandpower, Inc.
Attn: Kord S. Smith
504 Shoup Ave. 201
Idaho Falls, ID 83402-3658

1 Richard Malenfant
339 Andanada
Los Alamos, NM 87544

1 MS 0361 Ronald Simonton (7004)
1 MS 0405 Jeffrey Philbin (12333)
1 MS 0727 Thomas Sanders (6020)
1 MS 0727 Tracy Dunham (6870)
1 MS 0771 Dennis Berry (6800)
1 MS 0771 John E. Kelly (6870)
1 MS 1136 Paul Pickard (6872)
1 MS 1136 Susan Longley (6872)
1 MS 1141 Edward Parma (6872)
1 MS 1141 Sharon Walker (6883)
1 MS 1141 Richard Coats (6883)
1 MS 1141 Daniel Dorsey (6883)
1 MS 1141 Ronald Knief (6883)
1 MS 1141 Norman Schwers (6883)
1 MS 1142 James Bryson (6881)
1 MS 1142 Matthew Burger (6881)
1 MS 1142 Sidney Domingues (6881)
1 MS 1142 John Ford (6881)
1 MS 1142 Darren Talley (6881)
1 MS 1142 Robert Zaring (6881)
1 MS 1143 Ronald Seylar (6882)
1 MS 1143 James Andazola (6882)
1 MS 1143 Donald Berry (6882)
1 MS 1143 Francisco Gonzalez (6882)
1 MS 1145 Jack Loye (6880)
1 MS 1145 Theodore Schmidt (6880)
1 MS 1146 Kenneth Reil (6871)
1 MS 1146 Wu-Ching Cheng (6871)
1 MS 1146 Philip Cooper (6871)
1 MS 1146 Russell DePriest (6871)
1 MS 1146 Patrick Griffin (6871)
20 MS 1146 Gary Harms (6871)
1 MS 1146 Paul Helmick (6871)
1 MS 1146 S. Michael Luker (6871)
1 MS 1146 Brian Miller (6871)
1 MS 1146 Ahti Suo-Anttila (6871)
1 MS 1146 Donald King (6872)

1 MS 1146 Roger Lenard (6872)
1 MS 1146 Ronald Lipinski (6872)
1 MS 1146 Milton Vernon (6872)
1 MS 1146 Steven Wright (6872)
1 MS 9018 Central Technical Files (8945-1)
2 MS 0899 Technical Library (9616)

Blank Page